

# Opposing Effects of NGF and proNGF on HIV Induced Macrophage Activation

Kimberly S. Williams<sup>1,2</sup> · Deirdre A. Killebrew<sup>1,3</sup> · Gillian P. Clary<sup>1,4</sup> · Rick B. Meeker<sup>1,2</sup>

Received: 24 June 2015 / Accepted: 1 September 2015 / Published online: 29 September 2015  
© Springer Science+Business Media New York 2015

**Abstract** Macrophage and microglial activation by HIV in the central nervous system (CNS) triggers the secretion of soluble factors which damage neurons. Therapeutic approaches designed to restore cognitive function by suppressing this inflammatory activity have not yet been successful. Recent studies have indicated that the phenotype of macrophages is differentially controlled by the mature and pro form of nerve growth factor. These cells therefore may be highly responsive to the imbalance in pro versus mature neurotrophins often associated with neurodegenerative diseases. In this study we evaluated the interactions between neurotrophins and HIV induced macrophage activation. HIV stimulation of macrophages induced a neurotoxic phenotype characterized by the expression of podosomes, suppression of calcium spiking and increased neurotoxin production. The secretome of the activated macrophages revealed a bias toward anti-angiogenic like activity and increased secretion of MMP-9. Co-stimulation with NGF and HIV suppressed

neurotoxin secretion, increased calcium spiking, suppressed podosome expression and reversed 86 % of the proteins secreted in response to HIV, including MMP-9 and many growth factors. In contrast, co-stimulation of macrophages with proNGF not only failed to reverse the effects of HIV but increased the neurotoxic phenotype. These differential effects of proNGF and NGF on HIV activation provide a potential novel therapeutic avenue for controlling macrophage activation in response to HIV.

**Keywords** Inflammation · Neuroprotection · Calcium · Actin · p75 neurotrophin receptor · TrkA

## Introduction

Macrophages and microglia play a pivotal role in the development of HIV-associated neurological disease. Soon after HIV infection, activated monocytes infiltrate the central nervous system where they differentiate into perivascular macrophages with a relatively high viral burden (Fischer-Smith et al. 2008). Virus production within the CNS leads to chronic activation of infected and uninfected microglia and macrophages which, in turn, leads to secretion of neurotoxins (Giulian et al. 1990; Pulliam et al. 1991a; Kolson 2002). Much of the current work strives to develop strategies to reduce neural damage by suppressing the toxic activity of macrophages. This effort is complicated by the fact that macrophages are phenotypically dynamic cells that can secrete pro-inflammatory cytokines, anti-inflammatory cytokines, enzymes that modify extracellular proteins and/or growth factors depending on their external cues (Streit 2005). Thus, an understanding of the impact of the macrophage response to HIV must take into consideration both the positive and negative actions. This is important from a therapeutic perspective since

**Electronic supplementary material** The online version of this article (doi:10.1007/s11481-015-9631-z) contains supplementary material, which is available to authorized users.

✉ Rick B. Meeker  
meekerr@neurology.unc.edu

<sup>1</sup> Department of Neurology, CB #7025, University of North Carolina, 6109F Neuroscience Research Building, 115 Mason Farm Road, Chapel Hill, NC 27599, USA

<sup>2</sup> Neurobiology Curriculum, University of North Carolina, Chapel Hill, NC 27599, USA

<sup>3</sup> Present address: Center for Science and Mathematics Education, Stony Brook University, Stony Brook, NY 11794, USA

<sup>4</sup> Present address: US Food and Drug Administration, Rockville, MD 20852, USA

increasing evidence indicates that appropriate interventions may be capable of shifting the balance of activity to decrease damage while at the same time taking advantage of the macrophage's natural ability to protect and repair tissues.

Previous studies of cultured human monocyte-derived macrophages (hMDM) have shown that hMDM robustly express neurotrophin receptors TrkA and p75<sup>NTR</sup> and respond differently to their respective ligands mature nerve growth factor (NGF) and its precursor, proNGF (Williams et al. 2015). Exposure to NGF resulted in markedly different structural and functional phenotypes relative to proNGF, indicating that the peptides have distinct roles in the control of macrophage activation. NGF was shown to increase calcium spiking, membrane ruffling, phagocytosis and secretion of growth factors and other proteins beneficial for neuronal support. Stimulation with proNGF, in contrast, suppressed calcium spiking and increased podosome formation, migration and secretion of neurotoxins (Williams et al. 2015). Studies in HIV-infected humans have shown that neurotrophin levels are decreased in the brain compartment, suggesting a deficit in neurotrophin signaling (Meeker et al. 2011), a scenario similar to other neurodegenerative diseases such as Alzheimer disease where decreases in the ratio of NGF to proNGF correlate with disease progression (Al-Shawi et al. 2007; Mufson et al. 2007; Capsoni et al. 2011) (Kaul and Lipton 1999). The idea that alterations in neurotrophin signaling may contribute to degeneration in the diseased nervous system is supported by studies showing that neurotrophins and related ligands are protective in models of HIV-associated neuropathogenesis and Alzheimer disease (Mocchetti and Bachis 2004; Longo et al. 2007; Mocchetti et al. 2007; Yang et al. 2008; Shi et al. 2013). While neurons were the intended target cell in these studies, the subsequent demonstration of neurotrophin receptors on macrophages raised the possibility that an alteration in macrophage neurotrophin signaling may also contribute significantly to the disease process. Support for this possibility has come from studies of macrophages showing that NGF may increase CXCR4 expression, the receptor for SDF and co-receptor to HIV (Samah et al. 2008, 2009). While this might predict an increased susceptibility to infection, there is conflicting data on the role of NGF in HIV replication in macrophages (Garaci et al. 1999; Harrold et al. 2001; Samah et al. 2009). Known interactions of the HIV protein Nef in macrophages suggested activation of signaling pathways associated with podosome formation that might be similar to the recently described effects of proNGF (Verollet et al. 2015). In light of the potential interactions between neurotrophins and HIV pathogenesis we hypothesized that mature NGF might promote an anti-inflammatory, neuroprotective macrophage phenotype that counterbalances excessive inflammatory activation induced by HIV and/or proNGF. The following studies evaluated the ability of neurotrophin receptor stimulation to alter macrophage responses to HIV.

## Materials and Methods

### Isolation and Culture of Human Monocyte-Derived Macrophages

Human buffy coat leukocytes were purchased and shipped within 24 h after blood draw from healthy donors at the New York Blood Center (<http://nybloodcenter.org/>), a non-profit organization specifically for the collection and distribution of blood for clinical and research purposes. All research use was screened by the center and no personal identifiers were sent with the shipment. Such use is exempt from review under NIH guidelines, exemption 4 of 46-101 (b). Blood was diluted 1:1 with phosphate buffered saline (PBS) and was layered on top of Ficoll-Paque (GE Healthcare 17-1440-03). Blood/Ficoll-plaque was centrifuged at 500×g for 25 min and the peripheral blood mononuclear cells (PBMCs) were collected from the PBS/Ficoll-Paque interface. PBMCs were washed in red blood cell lysis buffer (Sigma R7757) to remove any red blood cell contamination. PBMCs were centrifuged at 450×g, the supernatant aspirated and the pellet resuspended in Dulbecco's modified eagle medium (DMEM) with high glucose, 10 % fetal bovine serum (Gibco 160000–044) and 20 µg/ml gentamicin (Gibco 15750–60). Cells were aliquoted into low adhesion 6 well plates (Corning 3471) at a density of approximately 10<sup>7</sup> cells/well. PBMCs were cultured for 5–7 days to allow monocyte attachment. Remaining white blood cells were washed, from the plate yielding a pure monocyte/macrophage culture. The adherent cells were differentiated into monocyte-derived macrophages using human GM-CSF (15 ng/ml) in complete DMEM for 1 week.

### Primary Cultures of Rat Forebrain

All animal work was done in accordance with NIH animal welfare guidelines and was approved by the University of North Carolina-Chapel Hill Institutional Animal Care and Use Committee board (approval number 14–147.0). Timed gestational embryonic day 9 (E9) pregnant female Long-Evans rats were delivered from Charles Rivers and allowed to rest in UNC animal husbandry until the time of experiments. At gestational day E17, rats were sacrificed by anesthetizing with isoflurane drop method until breathing and heart stopped. A thoracotomy was then performed prior to removal of the fetuses. For primary neuronal cultures, the uterus was briefly rinsed in 70 % ethanol and placed in HEPES-buffered Hank's balanced salt solution (HBSS) on ice before removal of the fetuses. The brain was removed from each fetus, extensively washed and the cortex/hippocampus was dissected from each brain and cleaned of dura-arachnoid membrane and visible vessels. The tissue was transferred to a 15 ml tube containing 5 ml calcium-magnesium free-HBSS + 2.4 U/ml dispase + 2 U/ml DNase

I and incubated for 25–30 min at 36 °C. Tissue was triturated and allowed to settle for 2 min. The suspended cells were transferred to a 50 ml culture tube containing 25 ml of minimum essential medium (MEM) with glutamine + 10 % fetal bovine serum + 20 µg/ml gentamicin. After several rounds of trituration in 2–3 ml calcium-magnesium free HBSS, dissociated cells were seeded at a density 20,000 cells/cm<sup>2</sup> on poly-D-lysine-treated coverslips for imaging and staining or 50,000–100,000 cells/cm<sup>2</sup> in 100 mm plastic dishes for Western blots. After 24 h, cultures were transferred to Neurobasal medium with B27 supplement. The resulting cultures were >95 % neurons at day 4 after seeding.

### Stimulation of Human Monocyte Derived Macrophages With HIV<sub>ADA</sub>

We obtained attenuated HIV<sub>ADA</sub> (CCR5 tropic) virions as a gift from Dr. Lishan Su. HIV virions were inactivated by aldrithiol (AT-2) (Rossio et al. 1998) and concentrated to 4.8 mg/ml. For stimulation, the virus was reconstituted in aCSF to a concentration of 100 ng/ml and then added to cultures at a 1:1000 dilution to achieve a final concentration of 100 pg/ml. This corresponds to a moderately high viral burden and was estimated to roughly correspond to 1–2 × 10<sup>6</sup> virions.

### Immunostaining

Differentiated hMDM grown on poly-D-lysine coated coverslips were transferred to DMEM containing 1 % FBS and stimulated for 1 h using four different conditions: Control (serum free DMEM), inactivated HIV, HIV + NGF human recombinant protein (100 ng/mL, Sigma N1408) or HIV + proNGF human recombinant protein targeted to high affinity sites (1 ng/ml, Alamone N-280). For inhibition experiments, hMDMs were stimulated with inhibitors of p75<sup>NTR</sup> (Ro-08-2750, 2 µM) or TrkA (GW441756, 100 nM) activation for thirty minutes prior to stimulation with the above conditions. The cells were gently washed and fixed in 2 % paraformaldehyde in PBS. Cells were washed 3 × in PBS and incubated in 3 % normal goat serum for 1 h. Incubation of primary antibodies was carried out overnight at 4 °C. Cells were stained using antibodies to: p75<sup>NTR</sup> (Millipore cat #07-476, 1:500), TrkA (Santa Cruz cat #SC-80961, 1:500) and sortilin (Millipore AB9712, 1:500). Cells were washed in PBS and incubated with species specific secondary antibodies conjugated to Alexa 488, 568 or 593 (Molecular Probes) in the dark for 1 h at room temperature. F-actin was stained using phalloidin Alexa488 or rhodamine (1:50, Molecular Probes) to show structural changes. Coverslips were then mounted using Fluoromount (Southern Biotech 0100–01) and digitally imaged on an Olympus XI71 microscope.

Analysis of stain intensity for individual cells or regions of interest within the cells was accomplished using Metamorph<sup>®</sup> software. Co-localization of p75<sup>NTR</sup> foci with TrkA or sortilin staining was analyzed by staining one receptor red and the other green followed by thresholding by intensity of stain, computer identification of stained objects and then documentation of each object's central X/Y coordinate for each wavelength. Objects with X/Y coordinates that overlapped within 0.46 µm were scored as co-localized. The analysis was restricted to outer portions of the cell where the stained features could be examined at high resolution.

### Co-immunoprecipitation

Human monocyte-derived macrophages in serum free DMEM were harvested from two 60 mm or one 100 mm dish using 1.5 ml lysis buffer (1X Ripa buffer (Thermo Scientific 89900), 1:100 phenylmethylsulfonyl fluoride (PMSF, Pierce Chemicals PI 36978), 1:100 Halt<sup>®</sup> protease inhibitor cocktail (Thermo scientific cat# 1861228). Protein concentration was measured by BCA assay (Thermo Scientific 23225). Fifty µl of agarose beads (Santa Cruz SC-2003) were added to 1 ml of protein lysate along with 10 µg of primary antibody (TrkA-Santa Cruz SC8096) and incubated overnight at 4 °C. Laemmli buffer (Bio-Rad 161–0727) was added in 1:1 proportion to beads and then boiled for 10 min. Immunoprecipitated protein was separated from the beads by collecting the supernatant. Protein lysate and immunoprecipitates were resolved on a TGX gel (Bio-Rad 456–1034) and transferred to a nitrocellulose membrane (Bio-Rad 162–0234). The membranes were blocked in 2 % milk plus 0.01% Tween for 1 h at room temperature. The primary antibodies were incubated overnight at 4 °C. The membranes were then washed in TBS+1 % Tween and incubated in secondary antibody for 1 h at room temperature. The membranes were then washed again and imaged using the film imaging system. The primary antibodies used were 1:500 p75<sup>NTR</sup> (Millipore 07–476). The secondary antibody used was 1:4000 Goat anti-Rabbit (Millipore AP132P). Film was processed using horseradish peroxidase (HRP) conjugated secondary antibody and SuperSignal West Pico detection (Thermo Scientific, #34080).

### Phagocytosis of Fluorescent Beads

Human hMDM were stimulated overnight in 1 % DMEM with HIV, HIV+ NGF or HIV + proNGF. Fluorescent 1 µm beads (Molecular Probes/Invitrogen F-8887) were placed into each well for 4 h at a concentration of 4.3 × 10<sup>5</sup> beads/ml. Excess beads not phagocytosed by hMDM were washed from the plate. The hMDM were stained with the live cell stain calcein AM (1 µM, 20 min) and digital images of the live cells captured at a magnification of 674 ×. Some cells were

then fixed in 2 % paraformaldehyde and stained with phalloidin-Alexa488 (1:50). Cells were individually traced and Metamorph software was used to measure the number of beads in each cell for each condition. The bead density was calculated by dividing the number of beads by the area of the cell. The average bead density was then calculated and compared between the treatment conditions.

### Transmigration Assay

Following an overnight stimulation of hMDMs with HIV, NGF+NGF or HIV+proNGF in DMEM with 1 % FBS, cells were harvested by incubating in ice-cold calcium-, magnesium-free HBSS for approximately 20–30 min to facilitate release of the hMDM from the low adhesion plate. Cells were washed from the plate with a 1 ml Rainin pipette using the flow of medium from the tip of the pipette to dislodge any remaining cells. The hMDM were centrifuged at  $80\times g$  for 5 min, the supernatant carefully aspirated and the soft pellet was re-suspended in DMEM containing 1 % FBS. The cells were counted and seeded into 8.0  $\mu\text{m}$  Matrigel invasion chambers (BD Biocoat cat# 354480) in the incubation medium at a density of  $10^5$  cells/chamber. Migratory behavior was measured by the number of cells entering the bottom chamber which also contained DMEM with 1 % FBS. Cells in the bottom chamber were labeled with the fluorescent live cell marker calcein AM (Life Technologies, C3100MP, 1  $\mu\text{M}$  20 min) and counted at 1 and 3 days after seeding.

### Flow Cytometry

PBMCs and hMDM were stimulated with HIV, HIV+NGF or HIV+proNGF in 1 % DMEM for 1 h. Cells were removed from low adhesion wells and centrifuged for 5 min at  $450\times g$ . Cellular pellets were re-suspended and fixed in a Fluorfix solution (Biolegend 420801) for 20 min at room temperature. Fixed cells were then treated with permeabilization buffer (E Bioscience 020-8333-56) and centrifuged for 5 min at  $450\times g$  at 4 °C. The cell pellet was re-suspended in permeabilization buffer and centrifuged at  $450\times g$  at 4 °C. Cells were re-suspended in 100  $\mu\text{l}$  of permeabilization buffer plus antibody (1.5  $\mu\text{l}$  p75; Alamone Labs ANT-007-F and 20  $\mu\text{l}$ ; TrkA R&D Systems FAB1715P; 5  $\mu\text{l}$  CD 206 Biolegend 321114; 5  $\mu\text{l}$  CD16 Biolegend 302008 and 5  $\mu\text{l}$  CD 163 Biolegend 333607) at room temperature for 20 min. The stained cells were washed three times in cell staining buffer (Biolegend 420201). Flow cytometry was performed on a FACS Calibur (Becton Dickinson, San Jose, CA) using direct immunofluorescence with at least 100,000 events. Monocytes were determined by populations of cells with high forward scatter and low side scatter. All cells were gated to remove debris. Three color staining analysis was utilized. Cells were analyzed according to side scatter and receptor bound fluorescence, and

data was collected with logarithmic amplifiers. Fluorescence spillover compensation was estimated using single-stained and unstained samples with the Cell Quest software (BD). After collection, data was further analyzed with FlowJo software (TreeStar Inc., Ashland, OR).

### Protein Profiles

Conditions for the analysis of secreted proteins were established to maximize the detection of toxic activity as described. For chronic exposure to HIV, the hMDM were stimulated for 3 days in 1 % DMEM with HIV, HIV+NGF or HIV+proNGF with daily neurotrophin addition. Medium was collected and centrifuged at 2500 rpm for 10 min to remove any floating cells in the medium. The cell free medium was added to a RayBiotech human antibody array L-507 and processed according to the RayBiotech Biotin Label-based human antibody array protocol. Slide arrays were scanned using an Agilent technologies DNA microarray scanner, and the analysis was carried out using Metamorph software. Internal negative controls were used to establish basal fluorescence and variation across the array. The minimum detectable fluorescence signal was set at 3.2 standard deviation units above the average background to give a probability of 0.001 that a protein signal would be identified as positive by chance. The linearity of signal detection was verified from internal positive standards. Since signal intensity varied between different arrays, protein expression was normalized to the total signal for all proteins on the array and expressed as a relative optical density value to indicate the strength of each signal. Expression of each protein was compared for HIV versus untreated controls. A comparison of HIV to NGF+HIV and proNGF+HIV was then run to determine if the pro and mature peptides interact differently with HIV. Proteins on the array that met the cutoff for a significant change were clustered into functional groups using DAVID software (da Huang et al. 2009a, b) and the relative enrichment of various functional classes determined taking into account the focused nature of the array. Based in part on this information, specific functional subgroups were analyzed in greater detail to determine which classes of proteins were preferentially modified by HIV in the presence or absence of NGF or proNGF.

### Neurotoxicity of Macrophage-Conditioned Medium

Pilot studies indicated that a 30 min stimulation of hMDM was sufficient to induce secretion of toxic factors which persisted for several hours after removal of the stimulus. Thus, the cells could be primed with neurotrophin, washed and the neurotrophin free medium subsequently tested for activity to eliminate any direct effects of the neurotrophins in the conditioned medium. For inhibition studies hMDMs were incubated with either p75<sup>NTR</sup> inhibitor (Ro-08-2750, 2  $\mu\text{M}$ ) or

p75<sup>NTR</sup> neutralizing antibody (EMD Millipore AB1554 1:500) or TrkA specific inhibitor (GW441756, 100 nM) for 30 min prior to stimulation with neurotrophins. Macrophages were stimulated with NGF or proNGF in serum free DMEM for 30 min. The medium was then replaced with serum free DMEM, the cells were challenged with HIV and the medium collected after 1 h. The macrophage-conditioned medium (MCM) was centrifuged at 2500 rpm for 10 min to remove any cells and then frozen in aliquots at  $-80^{\circ}\text{C}$ . The neurotoxic activity of the medium was tested on primary rat neurons cultured on coverslips. Neurons at 6–12 days in vitro were loaded with the calcium indicator, Fluo-4 AM (2  $\mu\text{M}$ , Molecular Probes, Inc., Eugene, OR) in aCSF (aCSF: NaCl 137 mM, KCl 5.0 mM,  $\text{CaCl}_2$  2.3 mM,  $\text{MgCl}_2$  1.3 mM, glucose 20 mM). For MMP-9 experiments, a specific MMP-9 inhibitor (MMP-9 inhibitor 1, 100nM) was added to neuron cultures in conjunction with Fluo-4 for 30 min prior to the analysis of the medium. After 30 min, the coverslip was transferred to a specialized stage for imaging. Cells were maintained in aCSF at  $25^{\circ}\text{C}$  and time lapse digital images were captured automatically by the Metamorph<sup>TM</sup> System. Images were captured every 6 s for 6 min to assess acute effects and every min for 60 min to assess delayed effects. Three pre-stimulation measurements were taken to establish basal levels of fluorescence at the beginning of each experiment. Neurons were stimulated with MCM at a 1:5 dilution. The increase in fluorescence intensity within each cell was then measured relative to the baseline fluorescence to correct for cell to cell differences in dye loading and intrinsic fluorescence. For most studies, cellular responses were averaged across all cells from at least triplicate runs to provide an indication of the “typical” response. In some cases individual cell response patterns are shown where the average masked important cell-specific profiles.

### Macrophage Calcium Activity

Macrophages cultured on coverslips were incubated with 100 ng/ml NGF or 1 ng/ml proNGF and the calcium indicator, Fluo-4 AM in aCSF for 30 min prior to imaging. Time lapse digital images were captured automatically every 6 s for 20 min by the Metamorph<sup>TM</sup> System. Three baseline images were captured followed by stimulation with HIV virions. Changes in fluorescence intensity within each cell were measured as described above.

### Statistical Analyses

Graphpad Prism software was used for data summaries and graphics. Parametric statistics were used to evaluate most changes induced by HIV  $\pm$  NGF or proNGF. In cases where the data were not normally distributed non-parametric statistics were used. Means were calculated for at least three

replicate experiments and the standard error of the mean calculated. T-tests were used for paired comparisons, analysis of variance with repeated measures for temporal data and Chi-square for the analysis of cell populations. The statistical values in the text represent results from t-tests unless otherwise indicated. A probability of  $<0.05$  for rejection of the null hypothesis was considered significant.

Protein array data was analyzed in a stepwise fashion with increasing stringency. First, negative controls on the arrays were used to establish variation within the array. A value 3.2 standard deviation units above and below the mean was calculated and represented the threshold values for a significant increase or decrease. This set the confidence limit at 0.001 so only one protein in 1000 would meet the cutoff by chance. The proteins that were significantly increased or decreased by these criteria were then analyzed using DAVID software to identify functional groups. For comparisons between two conditions, a linear regression analysis was performed to provide an index of how well the arrays matched. This analysis assumed that the majority of proteins on the array would not be changed by the challenge. The data fit this assumption well with all correlations exceeding an  $r$  value of 0.9. Proteins that deviated from the linear regression could then be identified on scatter plots as well as by the differential expression between challenge and control conditions. To increase the stringency we then asked how well the changes in protein expression could predict the neurotoxicity of the medium using the maximum delayed increase in intracellular calcium. A cutoff was arbitrarily set at a correlation of 0.7071 reflecting a relationship that accounted for approximately 50 % of the variability.

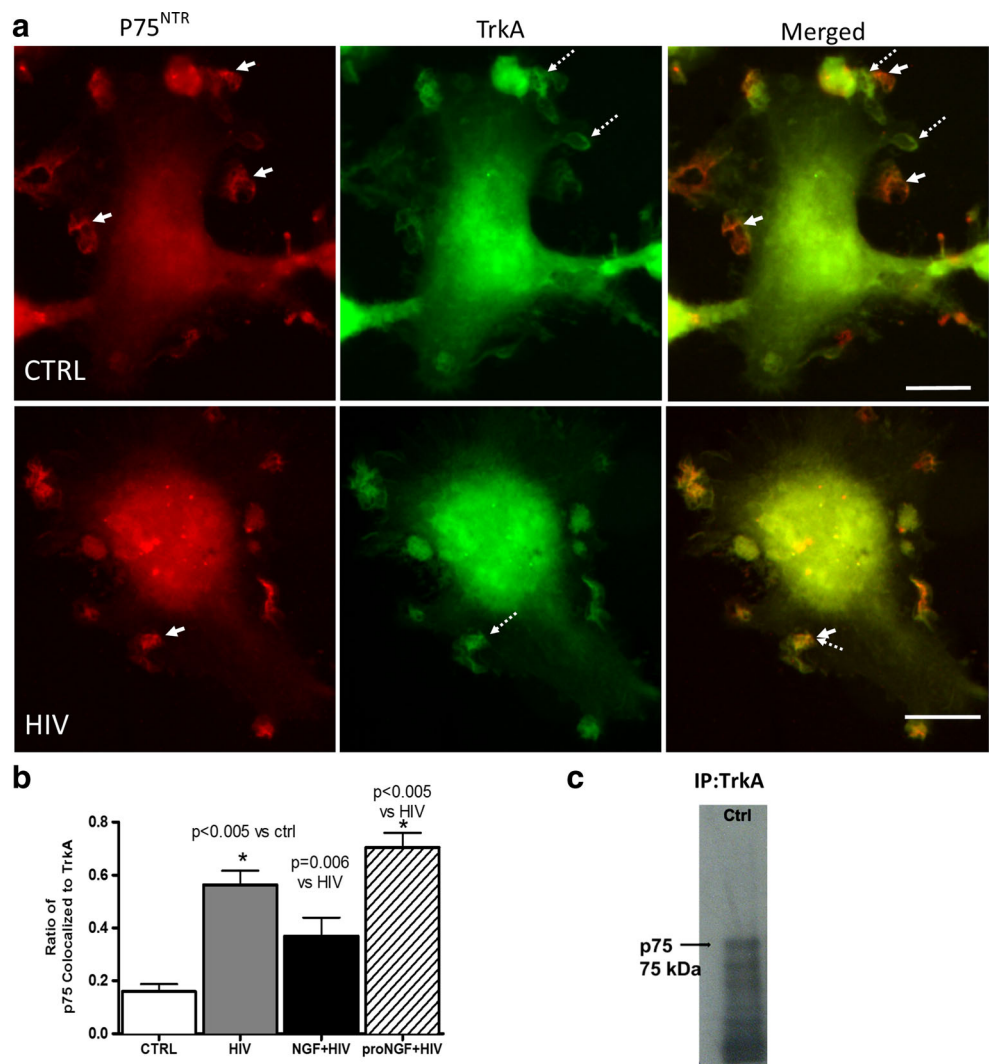
## Results

### p75<sup>NTR</sup> and TrkA Expression in Response to HIV

The neurotrophin receptors p75<sup>NTR</sup> and TrkA have recently been shown to be robustly expressed on hMDM and monocytes (Williams et al. 2015). To assess whether HIV could regulate the expression of p75<sup>NTR</sup> and TrkA, hMDM were exposed to HIV virions for 1 h followed by flow cytometry analysis. Exposure to HIV virions for 1 h failed to significantly influence the expression of p75<sup>NTR</sup> ( $45.2 \pm 8.5\%$  of cells, 82.7 % of control expression,  $p=0.08$ ) or TrkA ( $11.6 \pm 2.0\%$  of cells, 87.3 % of control expression,  $p=0.3$ ). Monocytes showed a similar profile and exposure of HIV virions for 1 h did not change p75<sup>NTR</sup> or TrkA expression.

Consistent with data from neurons showing that these receptors normally interact to influence the efficiency of TrkA signaling (Reichardt 2006), we confirmed sites of regional colocalization of p75<sup>NTR</sup> and TrkA within individual hMDM double stained for p75<sup>NTR</sup> and TrkA in ruffled regions of the cell (Fig. 1a). This overlap was not seen in all foci (Fig. 1a,

**Fig. 1** TrkA and p75<sup>NTR</sup> interactions in hMDM are increased by HIV. **a** Example of focal immunostaining for p75<sup>NTR</sup> (red) and TrkA (green) in control hMDM (CTRL) and hMDM treated with HIV. In control MDM, p75<sup>NTR</sup> (solid arrows) and TrkA (dashed arrows) are seen in separate regions with some overlap (yellow areas in merged image). HIV treatment increased the regional overlap of p75<sup>NTR</sup> (arrow) and TrkA (dashed arrow). Scale bar=25 μm. **b** Morphometric measurements of the overlap of p75<sup>NTR</sup> with TrkA showed an increase in the presence of HIV (\**p*<0.005 vs control) NGF co-stimulation with HIV reduced TrkA/p75<sup>NTR</sup> overlap compared to HIV treated hMDM (*p*=0.006) while proNGF synergistically increased the HIV effect (*p*<0.005 vs. HIV). Values are mean±sem, *n*=5 experiments. **c** The interaction of TrkA with the p75<sup>NTR</sup> was confirmed by co-immunoprecipitation. TrkA was immunoprecipitated from hMDM lysate followed by a Western blot for p75<sup>NTR</sup>. A 75 kDa band was identified with a p75<sup>NTR</sup> specific antibody



solid and dashed arrows). An average of 15.9±2.7 % of p75<sup>NTR</sup> and TrkA foci were overlapping in unstimulated cells with a resolution of 0.46 μm (Fig. 1a CTRL, and b). HIV stimulation increased the overlap of p75<sup>NTR</sup>/TrkA foci to 56.4±0.5 % in hMDM (Fig. 1a, HIV and b; *p*<0.001), indicating that HIV exposure induced a translocation of the receptors into overlapping domains. At the cellular level, flow cytometry analysis demonstrated that 71.0 % of TrkA expressing hMDMs co-expressed p75<sup>NTR</sup>, however, exposure to HIV for one day did not affect the proportion of cells co-expressing TrkA and p75<sup>NTR</sup> (65.5 % p75<sup>NTR</sup>/TrkA<sup>+</sup>) indicating that the increased overlap was not due to changes in receptor content. We also confirmed the interaction of p75<sup>NTR</sup> and TrkA by immunoprecipitating hMDM protein lysate with a specific TrkA antibody. A 75 kDa band was identified in the Western blot of the immunoprecipitated complex confirming that TrkA formed complexes with the p75<sup>NTR</sup> (Fig. 1c).

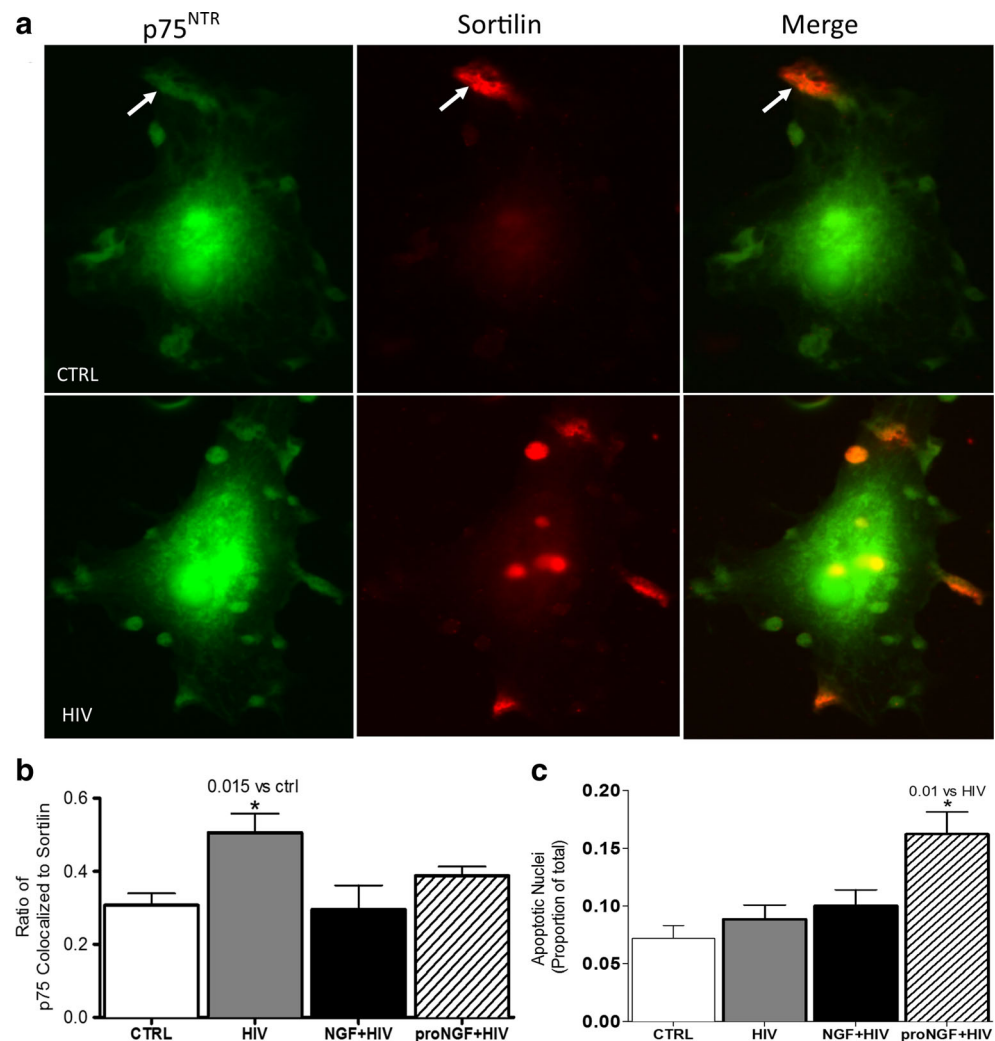
In previous studies, stimulation of hMDM with NGF greatly increased the co-localization of p75<sup>NTR</sup> and TrkA. To

determine if HIV altered the ability of the neurotrophins to influence the receptor association we also measured overlap of p75<sup>NTR</sup> with TrkA<sup>+</sup> foci after co-stimulation with HIV+NGF or HIV+proNGF (Fig. 1b). When compared to HIV, the p75<sup>NTR</sup>/TrkA overlap was reduced by 34.6 % for NGF+HIV (*p*=0.006) and increased 47.7 % for proNGF+HIV (*p*=0.002) indicating a small synergistic relationship with proNGF and antagonistic relationship with NGF.

### HIV Increased p75<sup>NTR</sup> and Sortilin Co-localization

Because of the relatively robust expression of p75<sup>NTR</sup> on the macrophages, we examined the expression of other receptors known to partner with p75<sup>NTR</sup>. Sortilin, a well known signaling partner with p75<sup>NTR</sup>, was also expressed at high to moderate levels in 43 % of hMDM (Fig. 2a). Sortilin foci were located in similar domains and overlapped with 30.7±0.3 % of the p75<sup>NTR</sup> foci (Fig. 2b). HIV had no effect on sortilin expression but induced a small 39.3 % increase in the overlap

**Fig. 2** HIV increased p75<sup>NTR</sup> co-localization with sortilin receptor but did not cause cell death. **a** Example of focal immunostaining highlighting the overlap of p75<sup>NTR</sup> (green) and sortilin (red) foci in control and HIV treated hMDM. Sortilin staining was seen in discrete foci which occasionally overlapped (arrows) with p75<sup>NTR</sup> in control hMDM. Treatment with HIV increased the extent of co-staining with multiple overlapping foci. **B.** HIV increased the overlap of p75<sup>NTR</sup>/sortilin immunostained foci in hMDM. HIV co-stimulation of hMDM with NGF or proNGF did not affect this p75<sup>NTR</sup>/sortilin overlap (\* $p=0.015$ ,  $n=5$  experiments). **c** Measurement of condensed and/or fragmented nuclei in bisbenzimidate stained hMDM showed few apoptotic cells with no change after exposure to HIV or 100 ng/ml NGF+HIV. Treatment with 1 ng/ml proNGF+HIV induced a small increase in apoptotic nuclei (\* $p<0.01$ ,  $n=12$  cultures). Values are mean $\pm$ sem



of p75<sup>NTR</sup> stained foci with sortilin (Fig. 2b;  $p=0.015$ ). Addition of NGF with HIV reduced the co-localization of sortilin with p75<sup>NTR</sup> back to control levels, but results were variable and the difference did not reach significance. Addition of proNGF with HIV had an intermediate result which was also not significant (Fig. 2b). These data indicated that although HIV did not alter p75<sup>NTR</sup> and sortilin expression, it fostered interactions between these receptors, creating an optimal environment for pro-neurotrophin signaling.

Since signaling of pro-neurotrophins through the p75<sup>NTR</sup> and sortilin receptor can promote cell death (Lee et al. 2001; Ibanez 2002), we stimulated hMDM overnight with HIV, 100 ng/ml NGF+HIV or 1 ng/ml proNGF+HIV and then stained with the dead cell marker ethidium homodimer. Dead cell nuclei were counted and the cells were fixed in 2 % paraformaldehyde followed by staining with the nuclear stain bisbenzimidate to identify all nuclei as well as apoptotic nuclei. No difference in dead cells was seen with ethidium bromide staining under any treatment conditions (10–12 % of total nuclei). Condensed and/or fragmented nuclei stained with

bisbenzimidate accounted for 7–10 % of all stained nuclei in unstimulated hMDM cultures and did not change in response to HIV or NGF+HIV (Fig. 2c). Cultures co-stimulated with proNGF+HIV showed a small but significant increase to 16 % ( $p=0.01$  vs HIV). This indicated that while HIV does not cause cell death in hMDM it may synergize slightly with proNGF to induce apoptosis in a small number of cells (6 %).

### HIV Suppressed Macrophage Calcium Activity

Macrophages in culture show a low intrinsic rate of small calcium spike generation which is increased by NGF and decreased by proNGF (Williams et al. 2015). HIV interactions with chemokine receptors have been shown to increase intracellular calcium in cultured human macrophages (Del Corno et al. 2001) although the temporal pattern of calcium spiking was not evaluated. To better understand the effects of HIV on intrinsic calcium activity we loaded hMDM with Fluo-4 and measured intracellular calcium at 6 s intervals over a 20 min period. The average calcium response showed that HIV

induced a small acute response not seen in control hMDM. However, control hMDM (aCSF) showed a small, gradual accumulation of intracellular calcium over the 20 min interval, which was suppressed by HIV. Addition of NGF (HIV+NGF) restored the calcium accumulation to near normal levels whereas proNGF (HIV + proNGF) suppressed calcium levels in the hMDM (Fig. 3a). These average responses, however, masked the presence of small intermittent calcium spikes, which were highly sensitive to the effects of HIV and the neurotrophins. See Fig. 5a–d and supplemental video 2 for examples of spiking in hMDMs. Calcium spike patterns are also illustrated in Fig. 3b which shows the composite activity of 10 adjacent cells. The plots provide a representative view of the typical responses under each condition and illustrate the lack of synchronization of the spike patterns. Untreated hMDM had an average intrinsic spiking rate of  $0.263 \pm 0.025/\text{min}$  (Fig. 3c). This was a slight underestimate of the actual rate in active cells since only 76 % of the cells showed

significant spikes. Exposure to HIV virions decreased the average spike rate to  $0.088 \pm 0.011/\text{min}$  ( $p < 0.001$ ). This was due to both a decrease in the spike frequency and number of cells that showed spiking behavior (46.4 %). This suppression was completely reversed when HIV was added in the presence of NGF ( $0.382 \pm 0.091$  spikes/mins;  $p < 0.001$ ). ProNGF+HIV was not significantly different from HIV alone although many cells showed a very strong suppression of spiking (Fig. 3c). These data suggest that HIV suppresses calcium spiking in hMDM and NGF, but not proNGF, can restore calcium activity.

### Modification of Macrophage Structure

Because of the mobility and diverse phenotypes of macrophages, the regulation of actin structures is extremely important. Previous studies have shown that NGF and proNGF induce very different structural phenotypes ranging from a

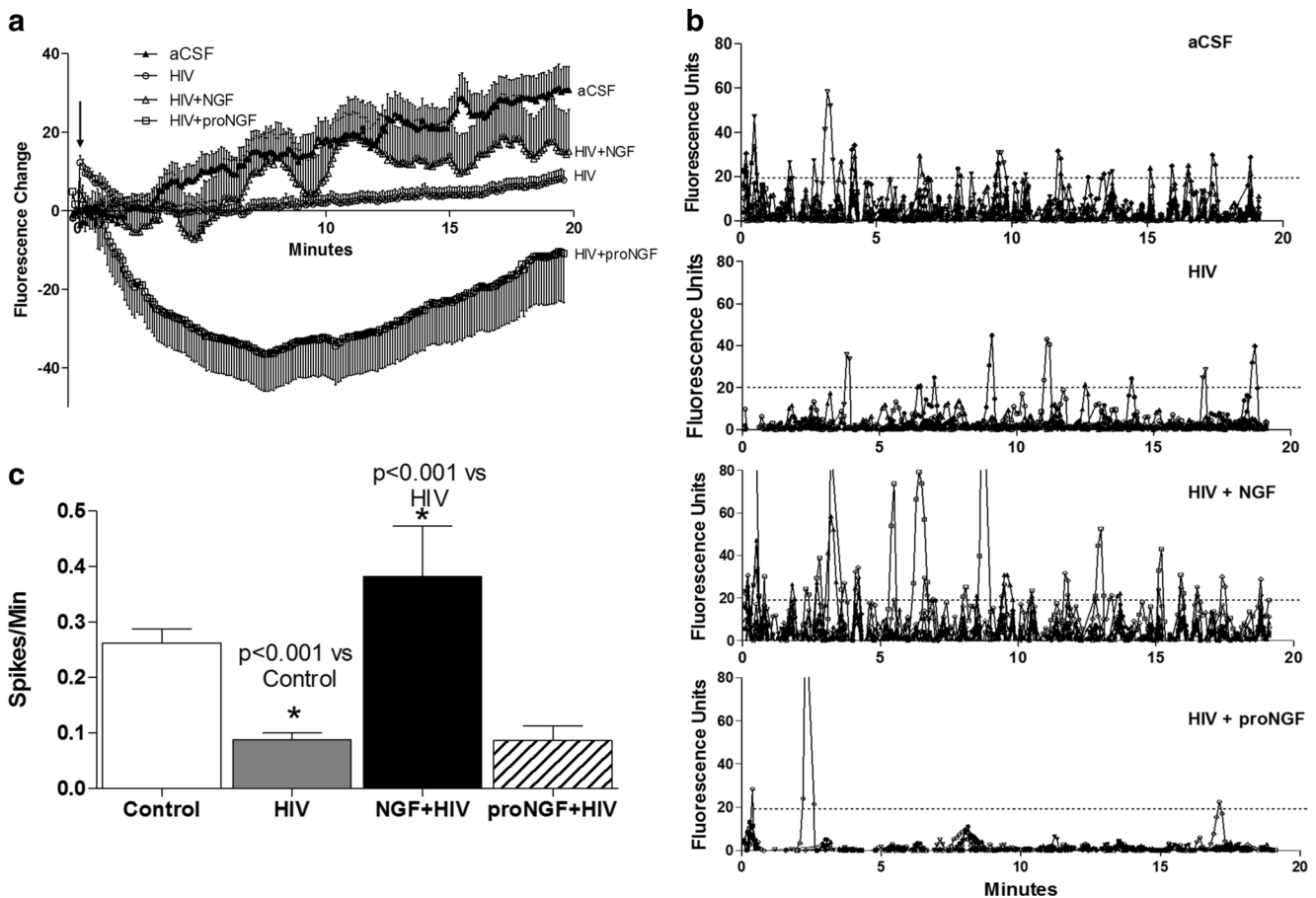


**Fig. 3** HIV and neurotrophins altered the pattern of calcium responses in hMDM. **a** Mean changes in intracellular calcium in hMDM. Treatment with HIV virions resulted in a small acute increase in calcium (arrow) not seen in vehicle treated hMDM (aCSF). HIV suppressed the gradual increase in average intracellular calcium levels seen in vehicle treated hMDM (aCSF). Addition of NGF to the HIV challenged hMDM partially restored the calcium accumulation whereas proNGF+HIV provoked a large decrease in calcium. **b** Examples of the spiking

patterns for a composite of 10 cells treated with aCSF, HIV, NGF+HIV or proNGF+HIV. HIV decreased the number of spikes that met the spike threshold criterion (dashed line). HIV+NGF increased the frequency of spikes whereas a low frequency of spikes was seen with HIV+proNGF. **c** Average spike frequencies were greatly suppressed by HIV ( $p < 0.001$  vs control). Suppression was completely reversed by co-stimulation with NGF ( $p < 0.001$  vs HIV,  $n = 10$  experiments) but not proNGF. Values are mean  $\pm$  sem



highly ruffled morphology at one extreme to flat macrophages expressing dense podosomes and no ruffles at the other extreme. To assess changes in these structures induced by HIV, cultured hMDM were exposed to HIV virions in serum free medium for 1 h, rapidly fixed with 2 % paraformaldehyde and stained with phalloidin-Alexa 488 or rhodamine to visualize F-actin. Under these conditions, untreated macrophages displayed a mix of morphologies at 1 h with  $37.0 \pm 5.1$  % possessing ruffles (Fig. 4a- Ruffled),  $22.9 \pm 3.0$  % podosomes (Fig. 4a- Podosome) and  $40.1 \pm 4.6$  %, with no distinctive specializations (Fig. 4a- No Specialization). These structures are highly dynamic as illustrated in the supplemental video 1 of a normal macrophage in culture (Supplemental movie 1). HIV stimulation for 1 h increased the relative number of macrophages possessing podosomes (55.9 % increase,  $p=0.03$ ) relative to the untreated cells (Fig. 4b). This HIV induced increase in podosome formation was restored to control levels by NGF ( $p=0.03$  vs. HIV), but not proNGF (Fig. 4b).

Many of the podosome rich cells also exhibited an increased polarization of the podosomes based on a five point

scoring system ranging from a uniform distribution of podosomes (1 = no polarization) to a large collection of podosomes restricted to one quadrant of the cell (5 = high polarization). An example of a polarized cell with a score of 5 is found in Fig. 4a-Polarized. Untreated macrophages had little podosome polarization ( $1.32 \pm 0.4$ , Fig. 4c) while HIV treated cells showed increased polarization ( $1.78 \pm 0.7$ ,  $p<0.001$ , 1 h). The increased polarization of podosomes by HIV at 1 h was reversed by treatment with NGF (Fig. 4c;  $p<0.001$ ), whereas, co-stimulation with proNGF + HIV slightly increased the degree of polarization over HIV alone (1.7 to 2.1,  $p=0.002$ ; Fig. 4c).

### Podosome Formation is p75<sup>NTR</sup>-Dependent

Since the HIV induced podosome expression was reversed by NGF, we evaluated neurotrophin receptor involvement in HIV induced podosome formation. Stimulation of hMDM with HIV resulted in an increase in the proportion of cells expressing podosomes (Fig. 4b and d). When the p75<sup>NTR</sup> was blocked

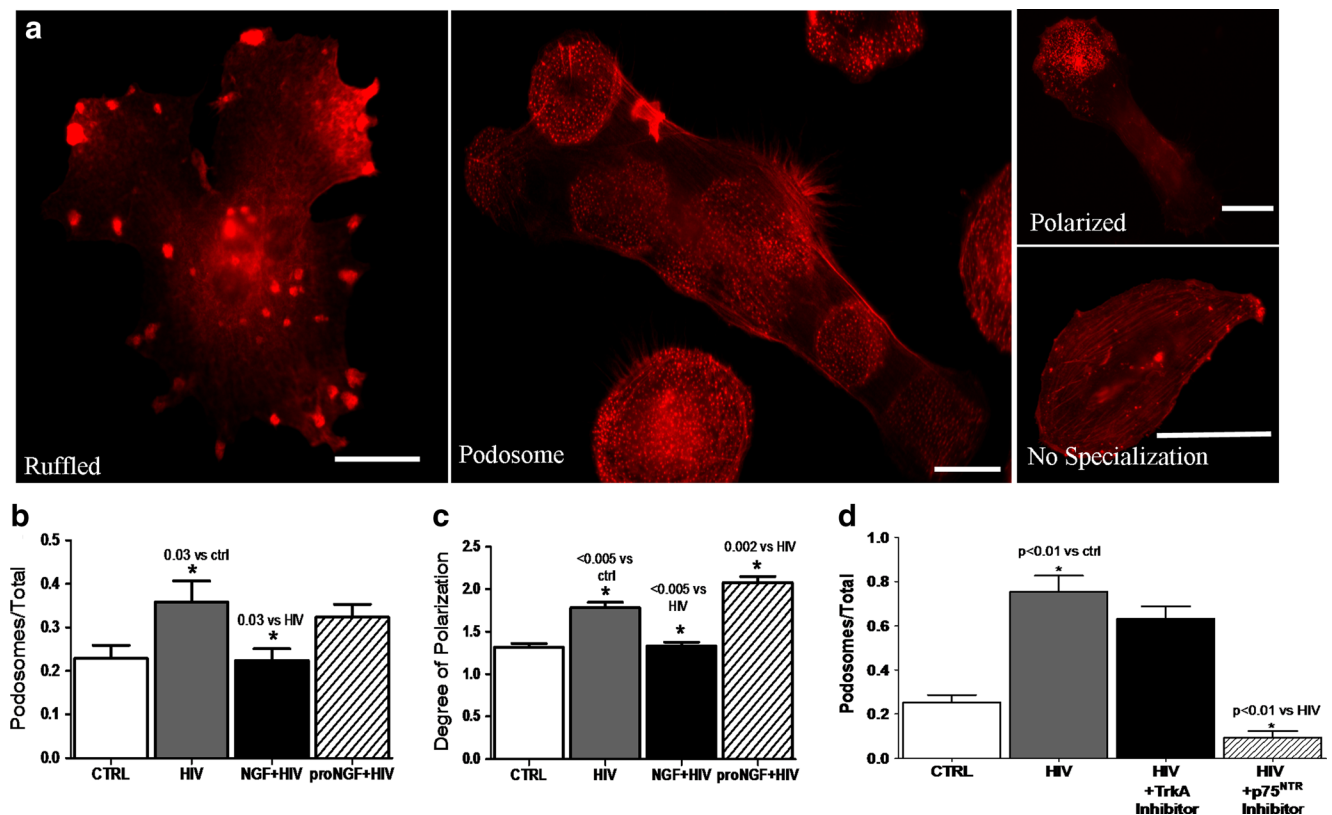


**Fig. 4** HIV induced podosome expression in hMDM. **a** Representative images of hMDMs stained for F-actin with phalloidin-rhodamine. Ruffled cells displayed distinctive foci of ruffled membrane. Podosomes typically appeared in cells with few ruffles and could be seen in clusters or throughout the cell. Clusters of podosomes were occasionally isolated in one quadrant of the cell (polarized). A subset of hMDM showed no distinctive specializations. A typical culture contained a mix of hMDM with ruffles or podosomes which shifted toward one phenotype depending on the stimulus conditions. **b** HIV increased the

relative proportion of hMDM expressing podosomes ( $p=0.03$  vs. control,  $n=20$ ). This effect was blocked by NGF ( $p=0.03$  vs. HIV,  $n=20$ ) whereas proNGF had no effect. **c** The degree of polarization of podosomes paralleled the podosome expression in **b** with HIV and proNGF+HIV showing increased polarization ( $p<0.005$ ,  $n=20$ ) and NGF+HIV reducing polarization ( $p<0.005$  vs. HIV,  $n=20$ ). **d** The HIV-induced increase in podosome expression was blocked by inhibition of the p75<sup>NTR</sup> ( $p<0.01$ ,  $n=10$ ) but not TrkA. Values are mean+sem

with a neutralizing antibody, not only was the effect of HIV blocked but the proportion of cells expressing podosomes was reduced below control levels to  $0.105 \pm 0.031$  (Fig. 4d;  $p < 0.01$ ). Blockade of TrkA with the specific inhibitor GW441756 did not have a significant effect on HIV-induced podosome expression ( $0.479 \pm 0.041$ , Fig. 4d). These data indicated that HIV induced podosome formation was dependent on  $p75^{\text{NTR}}$  signaling and not TrkA.

### Ruffled Cells Have Higher Spike Frequencies Than Podosome Bearing Cells

Since changes in structural phenotypes have been shown to correlate with changes in calcium responses, hMDM from eight experiments were segregated into groups by morphological phenotype (ruffled versus flat) and the corresponding calcium activity was evaluated. Calcium spikes were due to elevations in ruffled regions of the cells and well as the cell body. An example of macrophage calcium changes during a spike is illustrated in Fig. 5a–d. Also an example of moderate calcium activity in ruffled membranes is illustrated in the movie provided in supplemental video 2. On average, ruffled cells displayed 2.6 times the spike frequency of podosome bearing cells (Fig. 5e;  $0.287 \pm 0.043/\text{min}$  vs.  $0.108 \pm 0.022/\text{min}$ ,  $p < 0.001$ ), suggesting that the presence of ruffles but not podosomes correlated with calcium spiking.

### HIV Facilitation of hMDM Migration

Previous studies have shown that stimulation of macrophages with HIV protein, Nef induces podosomes and migratory activity (Verollet et al. 2015). Stimulation of hMDMs with HIV increased transmigration across a Matrigel coated transwell membrane by  $93.2 \pm 0.4\%$  compared to controls ( $p = 0.013$ ; Fig. 6a). Co-stimulation with NGF or proNGF did not have any effect on HIV induced migration.

### HIV Had no Effect on Phagocytic Activity in hMDM

Phagocytosis is one of the main functions of macrophages and has been correlated with cell ruffling (Ohsawa et al. 2004). Since HIV decreased the ruffled phenotype in culture we asked if it also suppressed phagocytic activity. One micron red fluorescent beads were added to macrophage cultures for 4 h to track phagocytosis. At the end of the 4 h period cells were stained with Phalloidin488. HIV stimulation did not alter the ability of macrophages to phagocytose the beads (Fig. 6b). However, NGF+HIV slightly reduced phagocytosis by 22.1 % compared to controls ( $p = 0.002$ ) and by 25.5 % compare to HIV alone ( $p < 0.005$ ). ProNGF+HIV had no effect on phagocytosis compared to control or HIV-treated cells. This result was counterintuitive since previous studies had shown that a more ruffled phenotype is associated with phagocytic activity (Williams et al. 2015). However, in the presence of

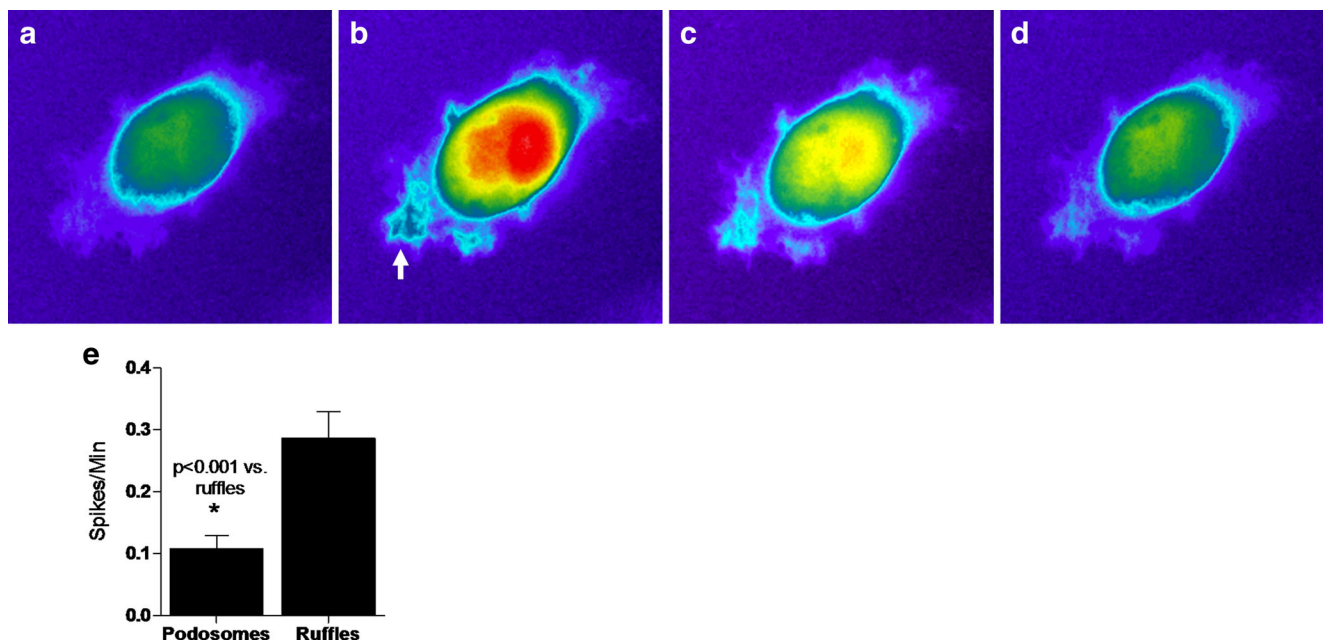


**Fig. 5** Ruffled cells have higher spiking frequencies than podosome bearing cells. **a–d** An example of a robust calcium spike seen in a normal hMDM. Pseudocolored images show a low level of resting calcium (**a**) which increases during a spike (**b–c**) and then returns to baseline (**d**). Calcium increases are seen in ruffled regions of the

membrane (*arrow*) as well as the cell body. **e** Measurement of intrinsic calcium spike frequency in cells expressing ruffles was significantly higher than cells expressing podosomes ( $p < 0.001$ ,  $n = 20$ ). Values are mean+sem

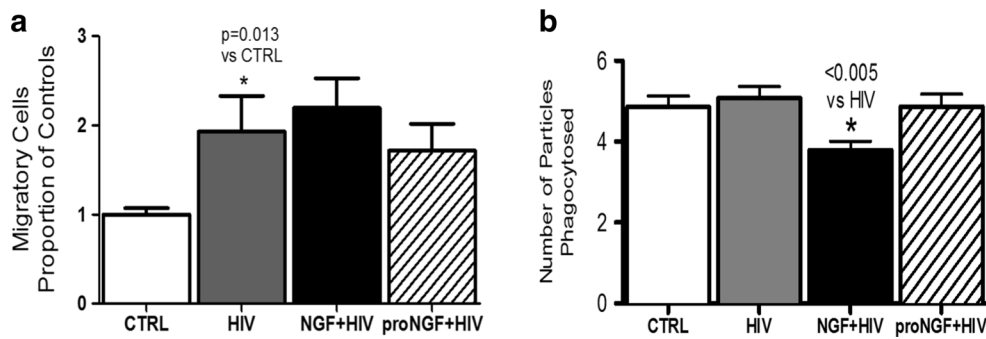


**Fig. 6** HIV increased hMDM migration but not phagocytosis. **a** hMDM exposed to HIV for one day increased the ability to migrate across a Matrigel barrier compared to untreated cells ( $p=0.013$ ,  $n=11$ ). The addition of NGF or proNGF did not affect HIV induced migration. **b**

Macrophages stimulated overnight with HIV±proNGF had no effect on phagocytosis. The addition of NGF with HIV slightly decreased phagocytic activity in cultures. ( $p<0.05$  vs. control) Values are mean±sem

HIV we noted that, while NGF reduced the number of cells with podosomes, a large number of cells lacked both podosomes and ruffles indicating only a partial reversal of the phenotype to an intermediate phenotype which may lack ruffles and phagocytic activity.

#### HIV Induction of Neurotoxin Secretion is Modulated by Neurotrophin Signaling

Secretion of unknown neurotoxins from macrophages in response to HIV has been strongly linked to neuronal damage. This neuronal damage includes dysregulation of calcium homeostasis and formation of varicosities along neuronal processes, often referred to as beading (Fig. 7a). To assess the generation of neurotoxic activity in the macrophage conditioned medium (MCM), hMDM were stimulated with HIV and conditioned medium was collected and added to primary rat neurons. Calcium accumulation was measured acutely over 6 min followed by assessment of the delayed calcium rise over a period of 60 min. Responses to HIV with or without neurotrophins were compared to control responses in the presence of vehicle (aCSF) or medium collected prior to the challenge. MCM from cells challenged with HIV virions induced a rapid increase in intracellular calcium that recovered partially during the acute phase and was then followed by a prolonged rise in calcium and subsequent formation of varicosities in the delayed phase. The time course of toxin release after stimulation with HIV showed a rapid release peaking at approximately 1 h followed by a relative stabilization of medium toxicity that lasted for at least 3 days (not shown). The rapidity of the response provided the opportunity to precondition the hMDM with neurotrophins followed by washout and 1 h of HIV stimulation. This washout protocol was important since any residual neurotrophins would be expected to have direct effects on the neurons. Therefore, hMDM were pretreated with NGF or proNGF for 30 min, washed and then stimulated for 1 h with HIV. When HIV was applied to hMDM pretreated with proNGF, a significant increase in the

toxicity of the MCM was seen based on both the level of calcium destabilization (Fig. 7b) and formation of varicosities (Fig. 7c). In contrast, MCM from cells treated with NGF followed by HIV showed partially reduced calcium dysregulation and beading. The slope of the delayed rise was almost flat indicating a lack of progressive calcium accumulation in the delayed phase. This data indicated that NGF and proNGF have opposing effects on the activation of the hMDM with NGF suppressing HIV-induced neurotoxicity and proNGF exacerbating damage.

To understand the role of neurotrophin receptors in HIV-associated neurotoxin production, TrkA was blocked with a specific inhibitor, GW 441756 and the p75<sup>NTR</sup> was blocked with an antibody to the extracellular epitope (EMD Millipore AB 1554; 1:500) or the inhibitor Ro-08-2750 before exposure to HIV virions (Fig. 8a). Toxic activity increased after blocking TrkA indicating a role for endogenous TrkA signaling in the suppression of toxin secretion. Blocking p75<sup>NTR</sup> with Ro-08-2750 or antibody both resulted in a small reduction in toxicity suggesting a limited direct role in toxic secretion.

Since all stimuli that led to the expression of podosomes were also associated with higher levels of medium toxicity, we compared the activity of MCM that was collected from unstimulated hMDM predominantly expressing podosomes or ruffles. MCM collected from hMDM with ruffles was consistently less toxic than MCM from macrophages with podosomes (Fig. 8b), providing support for a relationship between podosomes and macrophage toxicity.

#### HIV Induced a Complex Protein Secretory Profile Which Was Largely Reversed by NGF

Macrophages secrete a wide array of proteins in response to external cues that reflect the diversity of responses of these cells. To understand the full range of the secretory profile in response to chronic HIV exposure, we challenged the hMDM with HIV for 3 days. The medium was tested on primary

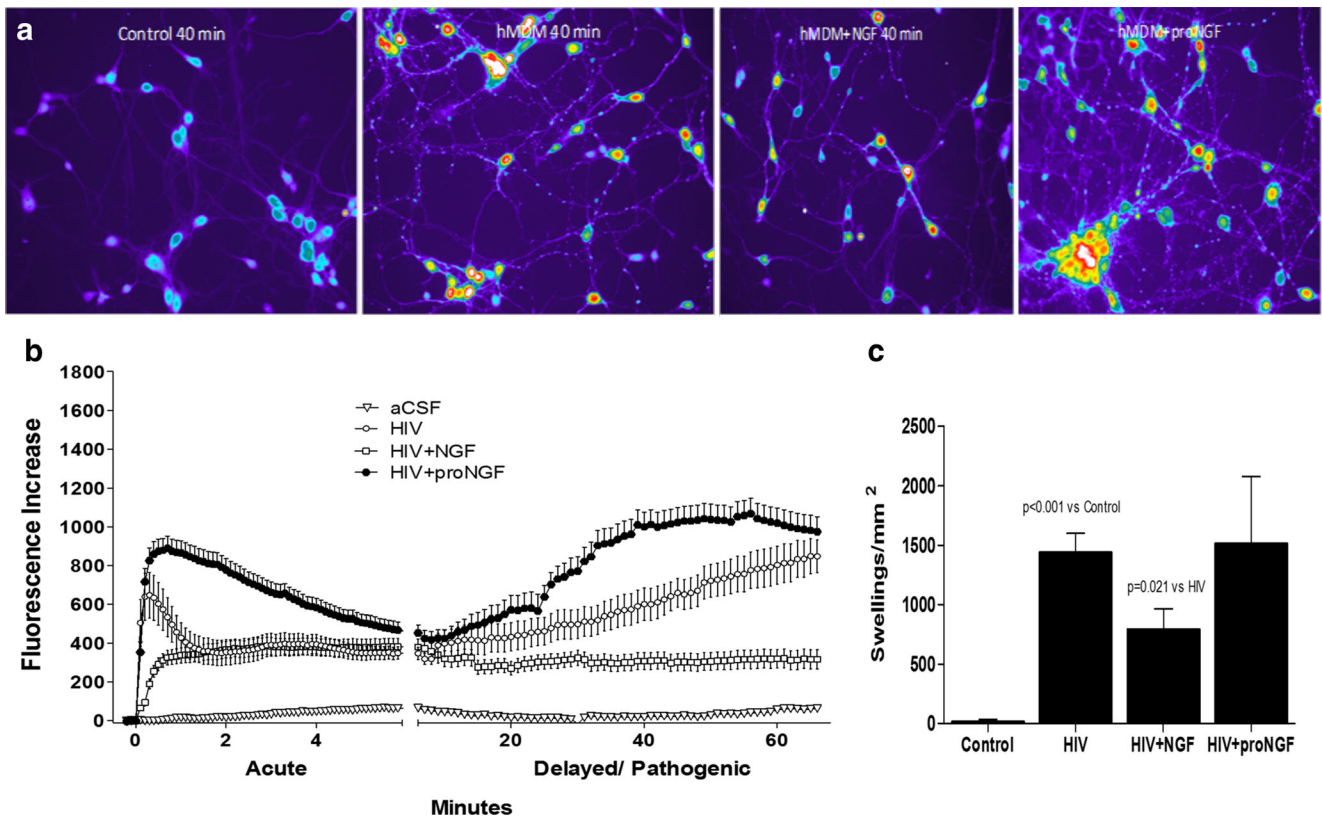


**Fig. 7** HIV induced neurotoxicity is increased by proNGF and partially suppressed by NGF. **a** An example of calcium levels and neuronal damage (beading) after 40 min treatment with conditioned medium from untreated macrophages (Control), HIV (hMDM), HIV+NGF (hMDM+NGF or HIV+proNGF (hMDM+proNGF)). **b** Average increases in intracellular calcium caused by macrophage conditioned medium. Conditioned medium from HIV stimulated macrophages

increased calcium influx acutely, followed by delayed calcium influx that persisted throughout the experiment. ProNGF increased the rate of calcium destabilization while NGF partially suppressed the delayed rise in calcium. **c** HIV increased the number of swollen varicosities ( $p < 0.001$  vs. control,  $n = 6$ ). ProNGF had no effect on HIV induced damage but NGF partially decreased beading formation ( $p = 0.021$  vs. HIV,  $n = 13$ ). Values are mean  $\pm$  sem

neurons to verify toxic activity and then analyzed in duplicate for cytokine, chemokine and growth factor content using the Ray Biotech L-Series Human Antibody Array L-507. Medium from the HIV challenged hMDMs was compared to MCM collected from the same cells just prior to treatment. Pre-treatment and post-treatment samples were tightly matched with correlations of protein content ranging from  $r = 0.982$  to  $r = 0.901$  indicating that most proteins did not change. Using the 99.8 % confidence limit as a cutoff, 13.3 % of the proteins (67 out of 503 proteins) assessed in this array were significantly changed by HIV (30 increased, 37 decreased). A summary of proteins changed by HIV, NGF+HIV or proNGF+HIV relative to controls is provided in Tables 1, 2, 3 and 4. Changes in the secretory profile of the hMDM in the presence of HIV are illustrated in the scatterplot comparing HIV to control values in Figure 9. The strong overall correlation ( $r = 0.901$ ) illustrated the consistency of the arrays with deviations from the line showing proteins that increased (above the line) or decreased (below the line) in the presence of HIV. Notable proteins increased by HIV included MMP-9, TIMP-1, MIP-2, MCP-1,

IL-8 and FGF-9. Notable decreases included ICAM-1, angiostatin, and thrombospondin.

To understand the functional impact of HIV on hMDM, proteins that increased or decreased were segregated into categories by function using the Database for Annotation, Visualization and Integrated Discovery (DAVID version 6.7; (da Huang et al. 2009a, b)), a bioinformatics tool. Six major functional groups were identified with the following Benjamini scores, in parentheses, reflecting strength of association: Immune response (8.1E-12), inflammatory response (2.1E-11), defense response (3.5E-11), chemotaxis (5.6E-11), response to wounding (1.8E-10), and regulation of cell proliferation (2.0E-9). Although the functional groups identified by DAVID were similar under all conditions, the analysis does not discriminate between increases and decreases. To provide a more detailed examination of the patterns of protein secreted after HIV exposure, the significant proteins were grouped into five major clusters that dovetailed with the functional groups identified by the bioinformatics analysis (growth factors, cytokines, chemokines, adhesion/MMP and other proteins) with

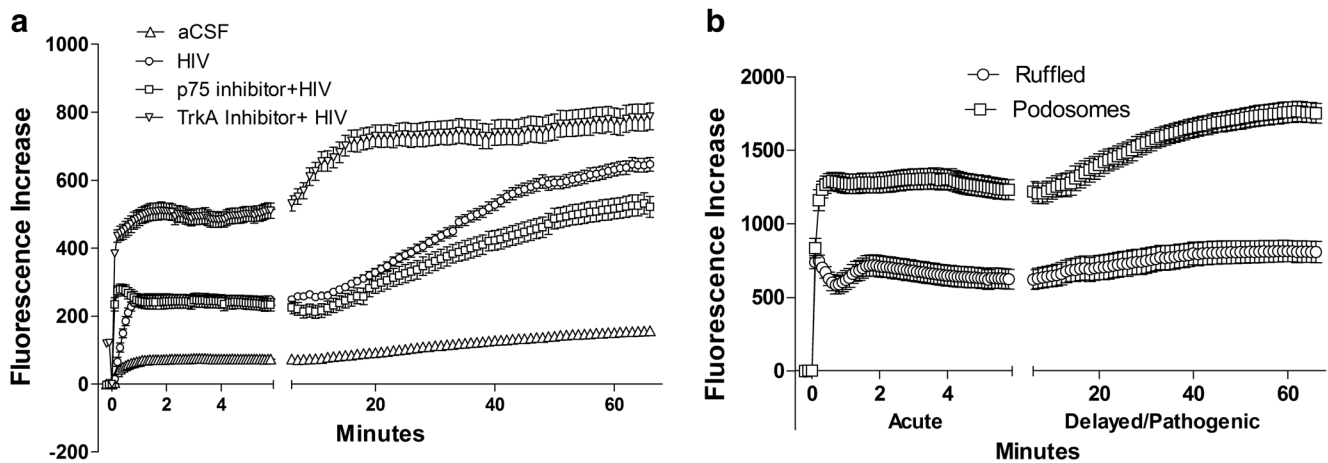


**Fig. 8** TrkA activity and membrane ruffling are associated with low neurotoxin formation. **a** Average calcium dysregulation caused by macrophage conditioned medium. Conditioned medium from HIV stimulated macrophages increased neuronal calcium influx acutely, followed by delayed calcium rise. Inhibition of TrkA signaling with the specific inhibitor GW441756 increased the level of calcium

destabilization. Blockade of p75<sup>NTR</sup> signaling with the inhibitor (Ro-08-2750) or a p75<sup>NTR</sup> neutralizing antibody decreased neurotoxicity. **b** Conditioned medium from cultures with mostly podosome bearing cells induced greater neuronal calcium destabilization than medium collected from cultures with ruffled cells. Values are mean±sem

up to nine functional families within each group. Within these groups the greatest changes were seen in proteins that regulate angiogenesis, growth, chemotaxis and inflammation.

One of the most notable changes following stimulation with HIV was within the family of angiogenic factors. Decreases in secretion were seen in factors that promote angiogenesis: angiopoietin and angiopoietin-like. A mixed response was seen in anti-angiogenic proteins with thrombospondin and thrombospondin-1 increased and angiostatin and thrombospondin-2 suppressed. Overall, this pattern indicated that HIV stimulation of hMDMs may encourage an anti-angiogenic like environment.

Other altered growth factors secreted in response to HIV largely belonged to the TGF and FGF families. HIV increased the secretion of TGF family proteins GDF3, GDF5, GDF15, Chordin like-2 and Activin RIIA but suppressed BMPR-1A and Activin A. In the FGF family, FGF9 and FGF13 were increased by HIV exposure while FGFR4, FGF11, and FGF16 were decreased.

Since macrophages are commonly categorized as classically activated (M1) or alternatively activated (M2) (Laskin et al. 2011), we examined markers typically used to distinguish these phenotypes. M1 markers were TNF- $\alpha$  IL-12p70, IL-6, IL-23, IFN- $\gamma$ , IL-1 $\alpha$ , $\beta$  and IP-10. M2 markers were IL-4, IL-10, IL-13, TGF- $\beta$  (1,2,3&5) and MCP-1. HIV increased the M1 marker IP-10 and M2 markers IL-13 and MCP-1. No other proteins classically associated with these activation states were influenced by HIV. We also evaluated changes in three cell surface markers of activation that had previously been associated with HIV infection and migration into the CNS: CD16 (M1), CD163 (M2) and CD206 (M2). Expression of CD16, CD163 or CD206 on both monocytes and

hMDM was evaluated by flow cytometry after 1 h exposure to HIV. HIV had no effect on the receptor expression of these markers on hMDMs. Although similar results were seen for the monocyte analysis, a subset of monocytes expressing high levels of CD206 (CD206<sup>high</sup>) were slightly decreased by HIV (−22.7 %,  $p=0.018$ ). However, a decrease was also seen with NGF+HIV (−33.4 % relative to control,  $p=0.04$ ) and HIV+proNGF (−60.7 %,  $p=0.006$ ) indicating the changes were independent of neurotrophin receptor stimulation. Thus, secretory profiles of hMDMs exposed to HIV did not reveal a clear M1 or M2 phenotype. Instead, a combination of inflammatory and anti-inflammatory cytokines was observed, highlighting the complexity of the macrophage response.

Lastly, proteins within the MMP family which regulate macrophage invasion and migration were among the more robust changes. HIV increased MMP-9 and tissue inhibitor of metalloprotease-1 (TIMP-1). These changes again indicated that hMDM responded to HIV by secreting both damaging proteins, such as MMP-9, and protective proteins, such as TIMP-1. Thus, there appears to be a constant balance of damaging and protective factors in an attempt to maintain homeostasis.

### NGF Reversal of the HIV Induced Secretory Profiles

Since previous studies indicated that neurotrophins altered proteins in the same functional groups as HIV (Williams et al. 2015), we anticipated that the effects of HIV might overlap with the neurotrophins. To analyze potential interactions, the HIV secretory response was correlated with the secretory response to HIV+NGF or HIV+proNGF.

**Table 1** Cytokine changes in hMDM medium in response to HIV, HIV+NGF or HIV+proNGF relative to medium from untreated control cells

Families	Subgroups	Protein Name	HIV minus Control	HIV+NGF minus CTRL	HIV+proNGF minus CTRL
Cytokine	TNF	BAFF R / TNFRSF13C	106	13327	406
		CD40 / TNFRSF5	-11340	-6544	-3945
		CD40 Ligand / TNFSF5 / CD154	-9665	-26365	-9743
		DR6 / TNFRSF21	-3187	-32806	-1360
		Fas / TNFRSF6	4706	-21303	3120
		Fas Ligand	306	14249	63
		GITR / TNFRF18	-1454	67837	-777
		Lymphotoxin beta R / TNFRSF3	-519	21483	81
		Osteoprotegerin / TNFRSF11B	-149	31859	1112
		TNF-alpha	-4400	-36167	-7035
		TNF RI / TNFRSF1A	106	12648	1734
	TNF RII / TNFRSF1B	263	15863	1159	
	Anti-inflammatory	B7-1 / CD80	-4667	11427	-5287
		CD 163	2138	-13447	4658
		Granzyme A	26226	-46366	36111
		HGFR	2419	-49563	-408
		IL-2	810	33225	1145
		IL-2 R alpha	1213	21762	2066
		IL-3	2039	20775	1489
		IL-3 R alpha	164	18096	-483
		IL-5	4891	-21298	4620
		IL-5 R alpha	-1767	29153	-88
		IL-9	-1012	-13834	-1664
		IL-15	10047	-22355	-3101
		IL-15 R alpha	-19659	-30459	-12974
		IL-16	-1169	12777	152
		IL-19	1631	28824	2047
		IL-20 R alpha	2511	20614	2856
		IL-22 R	-18851	-32827	-5978
		IL-24	-1614	57764	-390
		IL-28A	-646	33628	-1345
		IL-29	-14217	-1455	-9329
		MAC-1	-12227	-16109	-7499
		S100 A8/A9	2349	-15465	5507
		uPAR	-4916	14339	-5504
		IL-1 ra	-16038	1089	-23347
		IL-4 R	45779	-5097	84454
		IL-10	10058	-32122	4061
	IL-13	13340	-101679	-7266	
	IFN-alpha / beta R1	-680	17021	103	
	IFN-alpha / beta R2	-568	22858	170	
	IFN-beta	-890	15464	641	
Inflammatory	IFN-gamma	-158	14968	-179	
	IFN-gamma R1	-243	14050	372	
	IL-1 alpha	9421	-56567	-2808	
	IL-1 F5 / FIL1delta	596	13414	1407	
	IL-1 F8 / FIL1 eta	-20017	-29440	-14850	
	IL-1 R4 / ST2	-1016	17273	-807	
	IL-1 sRI	1098	28452	1874	
	IL-1 sRII	-545	11928	2855	
	IL-6	9926	-77545	-4774	
	IL-26	-5508	23208	-2308	
	IL-27	-1658	17273	-668	
	IP-10	11265	786	499	
	OSM	-27554	-97762	-19998	
sgp130	996	10741	-528		
IL-17	Galectin-3	-11800	-68003	-20596	
	IL-17B R	-1165	44852	-4660	
	IL-17C	-739	23117	-469	
	IL-17D	-1831	14098	-851	
	IL-17F	27543	14564	21993	
	IL-18 R alpha /IL-1 R5	-30292	-45219	-19414	
	IL-21 R	-761	43763	-591	
IL-23	-6346	79511	-5799		
IL-23 R	-750	41297	249		

Shaded values represent significant changes in protein secretion by HIV, NGF+HIV or proNGF+HIV relative to matched control medium. Proteins were analyzed on the Ray Biotech L-Series Human Antibody Array L-507. Values are expressed as relative fluorescence units

**Table 2** Chemokine changes in hMDM medium in response to HIV, HIV+NGF or HIV+proNGF relative to medium from untreated control cells

Families	Subgroups	Protein Name	HIV minus Control	HIV+NGF minus CTRL	HIV+proNGF minus CTRL
Chemokine	Chemokine	BLC / BCA-1 / CXCL13	-8015	19636	-2437
		CCL28 / VIC	-18558	-18810	4544
		CCR2	-866	13121	-415
		CCR4	-35225	-57182	-28281
		CCR7	-39192	-70605	-64016
		CCR9	-32106	-62681	-60976
		CTACK / CCL27	32895	7973	58913
		CXCL14 / BRAK	3255	10186	14003
		CXCR1 / IL-8 RA	3645	29852	12469
		CXCR2 / IL-8 RB	-43054	-87604	-70144
		CXCR4 (fusin)	-2386	25437	-1652
		CXCR6	1219	33873	979
		Eotaxin / CCL11	-3308	30576	-3580
		Eotaxin-2 / MIPF-2	-444	45573	939
		Fractalkine	-916	38976	-746
		GRO	1617	-120794	-25753
		GRO-a	508	30445	1232
		HCC-4 / CCL16	-5128	13128	-3516
		IL-8	57102	-54714	30797
		I-TAC / CXCL11	-15833	-736	-4994
		Lymphotactin / XCL1	-1151	12378	266
		MCP-1	67321	-91618	22672
		MCP-2	-354	15943	-1272
		MIG	25792	-94504	693
		MIP-1a	-1042	39685	-400
		MIP-1b	14233	-35464	23874
		MIP 2	49392	-138213	15954
		SDF-1 / CXCL12	-1559	11315	-1161
Tarc	-1837	26143	-236		

Shaded values represent significant changes in protein secretion by HIV, NGF+HIV or proNGF+HIV relative to matched control medium. Proteins were analyzed on the Ray Biotech L-Series Human Antibody Array L-507. Values are expressed as relative fluorescence units

Strong correlations were seen in both cases (0.951–0.956), indicating that changes were restricted to a small subset of proteins. Co-stimulation of macrophages with NGF in the presence of HIV normalized the expression of 58 out of 67 secreted proteins (increased or decreased) with a synergistic effect seen in only 2 proteins (Tables 1, 2, 3 and 4). In contrast, proNGF reversed changes in only 21 proteins and showed 11 synergistic effects with HIV.

To add an additional level of stringency we evaluated the ability of the protein changes to predict the calcium dysregulation seen in neurons under each condition by correlating the protein level to the average maximal delayed calcium response. A cutoff was arbitrarily set at a value that would account for approximately 50 % of the variation ( $r=0.7071$ ). Twenty six proteins met the dual criteria of a change in response to HIV and a moderately strong correlation with the toxicity profile. Proteins that showed a strong positive and negative correlation with toxicity are illustrated in Fig. 10a and b, respectively. Of these 26 proteins, NGF was able to reverse many of the HIV-induced profiles. The most notable proteins in the positive correlation group (reversal of HIV

increases, Fig. 10) were MMP-9, TIMP-1, erythropoietin, FGF-9 and IL-4R suggesting modulation of metalloprotease activity and growth.

Proteins with moderate positive changes included IL-17F, CTACK, IL-8, thrombospondin, GDF3, and the insulin receptor. Notable responses in the second group (reversal of HIV decreases, Fig. 10b) included angiostatin, CNTF, FGF-16 and ICAM-1 suggesting normalization of growth and adhesion functions. The potential role of the other proteins is less clear. Overall, these patterns indicate that NGF is a relatively strong antagonist of the effects of HIV, whereas, proNGF has less potent or even synergistic effects.

The large effects on MMP-9 and TIMP-1 secretion are particularly notable as MMP-9 is elevated in the CSF of patients with HIV infection and has been suggested as a potential neurotoxin (Conant et al. 1999; Liuzzi et al. 2000; Johnston et al. 2001; Russo et al. 2007). The normalization of both MMP-9 and TIMP-1 by NGF is consistent with a protective effect (Fig. 10a). In the presence of proNGF, an increase in MMP-9 and a corresponding decrease in TIMP-1 was seen which could help to explain the synergistic neuronal calcium

**Table 3** Growth factor changes in hMDM medium in response to HIV, HIV+NGF or HIV+proNGF relative to medium from untreated control cells

Families	Subgroups	Protein Name	HIV minus Control	HIV+NGF minus CTRL	HIV+proNGF minus CTRL
Growth Factors	VEGF	VEGF R2 (KDR)	-1006	15578	-885
		VEGF-B	-185	24580	-304
		VEGF-D	-13125	-17619	-5559
	TGF	Activin A	-20263	-14313	-17269
		Activin RIIA	14199	-26917	58291
		BMP-2	2089	-18782	-3551
		BMP-4	-1106	17694	-1332
		BMP-6	1236	35736	1560
		BMP-8	-5220	27063	-3348
		BMPR-IA / ALK-3	-13149	-3292	-12042
		BMPR-IB / ALK-6	-3347	17727	-6139
		BMPR-II	-2095	84432	-616
		Chordin-Like 2	21377	-31043	48721
		ErbB2	-548	17220	1354
		ErbB4	-1031	10504	-174
		Follistatin	-513	15944	2018
		Follistatin-like 1	2055	16792	6712
		GDF3	37468	-109106	28889
		GDF5	20089	-53913	17850
		GDF8	726	-31638	260
		GDF9	6574	-44318	3796
		GDF11	1268	32568	2147
		GDF-15	38494	-10924	12545
		Latent TGF-beta bp1	-784	11190	332
		Smad 4	1058	14593	2985
		TGF-beta 1	-8795	10700	-5210
	TGF-beta 2	231	27298	1293	
	TGF-beta 3	950	16394	1422	
	TGF-beta RII	-553	18616	37	
	Cerberus 1	-1155	11904	-279	
	DAN	-933	10396	169	
	EGF	Cripto-1	-1381	21350	1129
		HB-EGF	7775	-27029	-13674
		NRG3	-28587	-22487	-18529
		SMDF / NRG1 isoform	936	12687	1788
	Neurotrophin	BDNF	-8401	28255	-9141
		beta-NGF	-1838	23430	-283
		CNTF	-19306	-56721	-44125
		CNTF R alpha	-5053	12207	-2571
		GDNF	-681	14192	-644
		GFR alpha-2	-35235	-49205	-32253
		GFR alpha-3	-4996	-12598	-3955
	NT-4	-2303	14208	888	
	CSF	GCSF	3983	-55210	-5441
		G-CSF R / CD 114	-2864	15129	-2135
		GM-CSF R alpha	-2609	15045	424
		M-CSF R	-557	29322	2940
	IGF	IGFBP-2	-1080	13846	-1216
		IGFBP-3	-599	31266	72
		IGFBP-6	566	30717	-62
		IGF-I SR	233	28575	1508
	FGF	FGF Basic	7775	22852	1207
		FGF R4	-49276	-66523	-69610
		FGF-9	74890	-18032	52647
		FGF-11	-11998	-25905	-3011
		FGF-13 1B	16375	-20872	1045
		FGF-16	-14550	-25438	1512
		FGF-18	184	16444	836
	Angiogenic	Angiogenin	-3073	23646	2699
		Angiopoietin-1	-17080	-19004	-11899
Angiopoietin-like 1		-49282	-141003	-110478	
Angiopoietin-like 2		-7598	-11670	-9360	
Angiostatin		-54257	-128664	-13720	
Thrombospondin (TSP)		44047	11909	42308	
Thrombospondin-1		25437	-17421	4236	
Thrombospondin-2		-24096	-28032	-19596	
Tie-1	536	12093	2210		
Tie-2	111	19235	1648		

Shaded values represent significant changes in protein secretion by HIV, NGF+HIV or proNGF+HIV relative to matched control medium. Proteins were analyzed on the Ray Biotech L-Series Human Antibody Array L-507. Values are expressed as relative fluorescence units



**Table 4** Changes to MMPs and other proteins in hMDM medium in response to HIV, HIV+NGF or HIV+proNGF relative to medium from untreated control cells

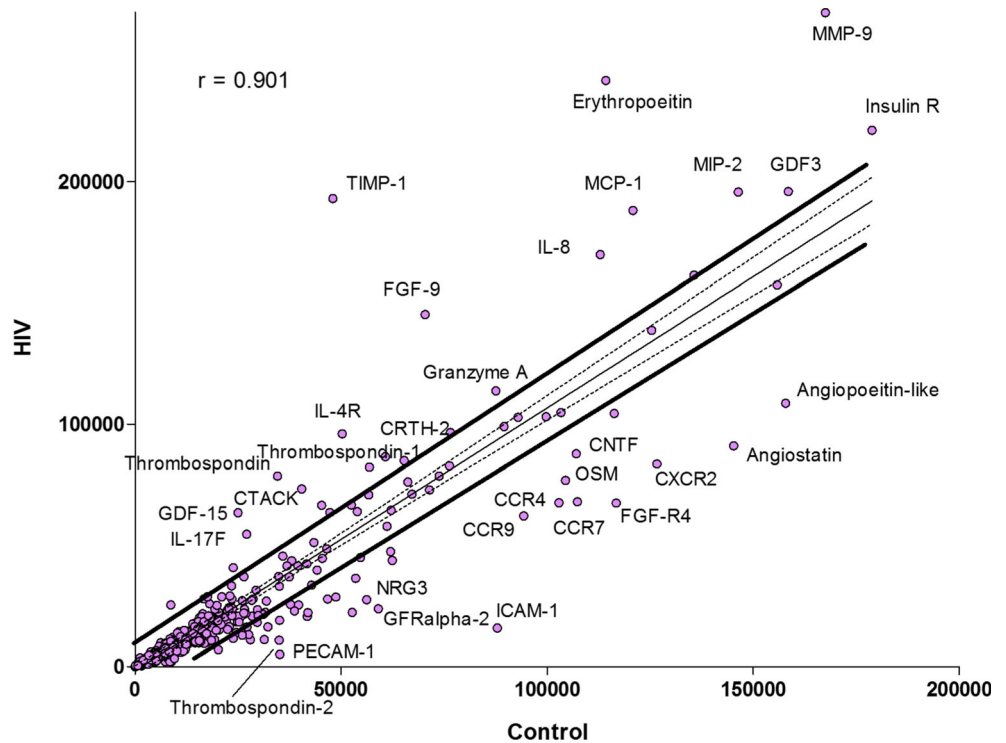
Families	Subgroups	Protein Name	HIV minus Control	HIV+NGF minus CTRL	HIV+proNGF minus CTRL
Other	MMP	MMP-1	310	26055	-115
		MMP-2	-566	10579	506
		MMP-7	2488	25959	1699
		MMP-9	102248	-131985	128646
		MMP-10	-547	10615	956
		MMP-12	2499	26071	4174
		MMP-14	-896	12530	-349
		MMP-24 / MT5-MMP	16827	-3206	-1368
		MMP-25 / MT6-MMP	-1457	-1462	-356
		TIMP-1	145157	-4189	65864
	TIMP-3	-952	10836	-491	
	Adhesion	E-Selectin	-452	-20434	2973
		ICAM-1	-72035	-74985	-33392
		ICAM-5	2057	-27117	-19847
		LFA-1 alpha	-1644	30936	-47
		PECAM-1 / CD31	-30058	-17302	8167
		Siglec-5 / CD170	-1769	12852	1588
	Siglec-9	-14322	992	-13727	
	MISC	ALCAM	-1791	14574	2449
		APJ	-2891	12528	-2046
		AR (Amphiregulin)	1062	12967	1400
		APRIL	3396	-28731	88043
		Artemin	123	45038	-2377
		Axl	474	12690	54
		BIK	-1189	13216	-781
		Coagulation Factor III / Tissue Factor	-10565	-9471	-11684
		CRTH-2	25855	-30722	-6070
		CTLA-4 / CD152	4561	16574	4225
		D6	-356	15459	-5
		EDA-A2	-15802	-22094	-11625
		EMAP-II	-9294	-16308	-9329
		EN-RAGE	16991	-5482	-1523
		Erythropoietin	127491	-66938	67874
		Frizzled-1	-2030	12149	-356
		Frizzled-7	-1748	11798	-119
		GASP-1 / WFIKKNRP	-21077	5333	-20815
		Glucagon	-782	29041	-3196
		Glut2	819	20346	1280
		GREMLIN	-9588	-10463	-9143
		Growth Hormone (GH)	1398	-62521	-2703
Growth Hormone R (GHR)		-1262	11438	349	
HCR / CRAM-A/B		-730	14270	-612	
Hepassocin		6179	-11897	-1418	
Inhibin B		2912	37089	1760	
Insulin R		42477	-123814	10739	
Kremen-1		-4371	11826	-2754	
LIF R alpha		10688	2428	-7603	
Lipocalin-1		5321	-10444	-8737	
MDC		-7676	18155	-8984	
Musk		-9152	-16464	-9911	
NeuroD1		582	10699	1135	
Orexin B		-1400	-11539	253	
Progranulin	19744	-54771	21624		
Prolactin	-10844	-17780	-10935		
SCF	74	10707	769		
SIGIRR	-16940	-23582	-10231		
SPARC	9826	-5679	10450		
Thrombopoietin (TPO)	98	11949	-1086		
Thymopoietin	-1183	10800	161		
TLR3	266	10515	-841		

Shaded values represent significant changes in protein secretion by HIV, NGF+HIV or proNGF+HIV relative to matched control medium. Proteins were analyzed on the Ray Biotech L-Series Human Antibody Array L-507. Values are expressed as relative fluorescence units

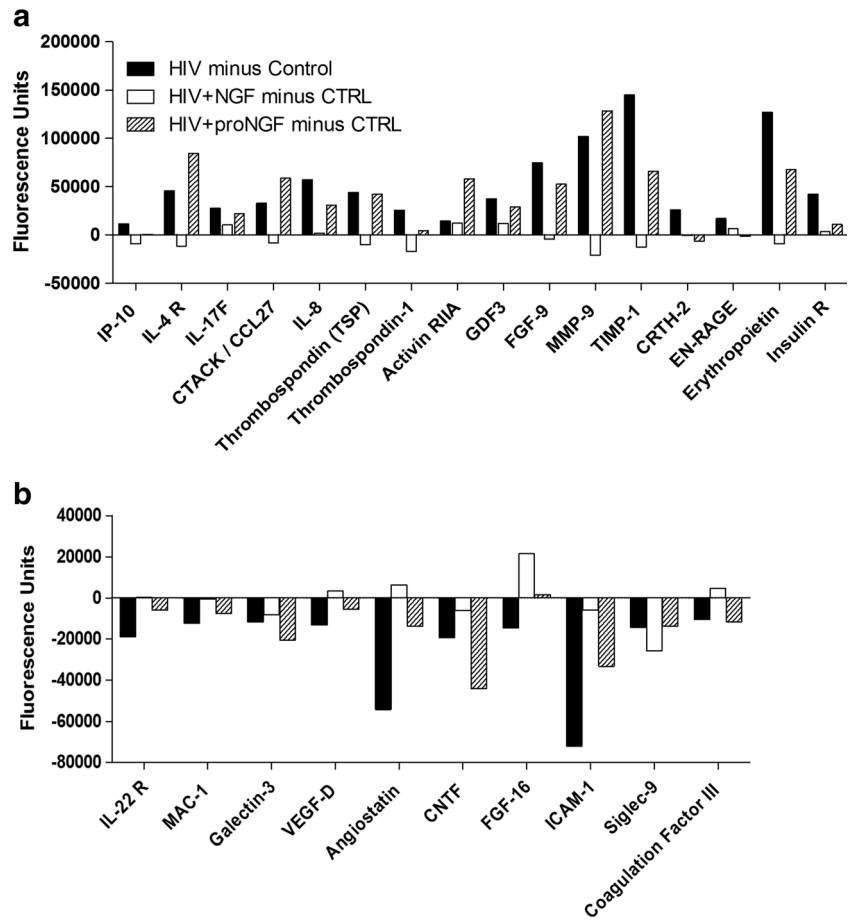
destabilization effects of proNGF with HIV stimulation. To better understand MMP-9’s role in neurotoxicity, we incubated MCM with a specific MMP-9 inhibitor and tested its ability

to induce calcium destabilization in rat cortical neurons. Normal conditioned medium from macrophages stimulated with HIV resulted in delayed calcium destabilization that was

**Fig. 9** Changes in the hMDM protein secretory profile induced by HIV. Values represent the correlation of changes in fluorescence signal intensity on the protein array for HIV versus untreated hMDM.  $r=$ the correlation coefficient. The solid line represents the 99.9 % confidence limits for the regression line. Proteins showing the greatest changes are indicated



**Fig. 10** Proteins in macrophage conditioned medium which correlated with the ability of the medium to induce calcium destabilization in cortical neurons. Values represent the change in fluorescence signal intensity on the protein array for HIV, NGF+HIV or proNGF+HIV treated cells relative to matched control medium collected prior to stimulation. To match the calcium profiles HIV had to produce an increase (a) or decrease (b), which was reversed by NGF and enhanced by proNGF. In each case the protein response pattern was matched to the calcium dysregulation. Proteins with  $r > 0.701$  (positive or negative) were considered to have a strong relationship to toxic activity and are presented in the figure



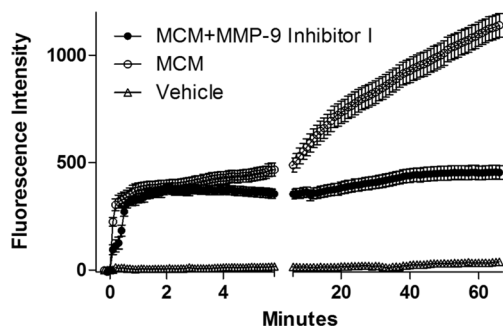
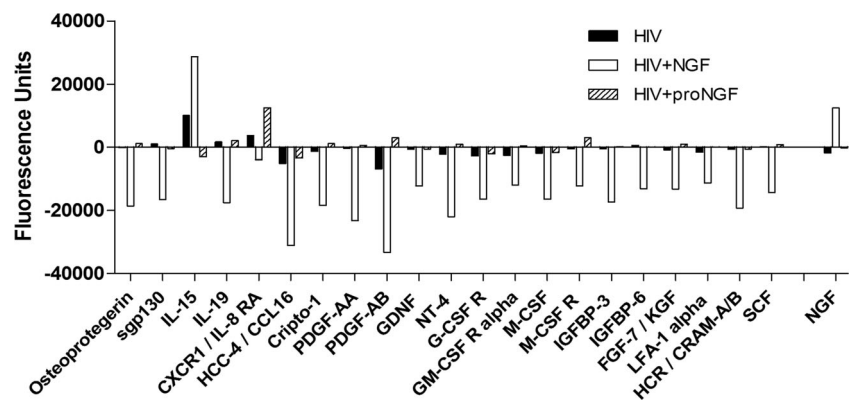


**Fig. 11** HIV induced neurotoxicity is suppressed by MMP-9 inhibitor I. A. Conditioned medium from HIV stimulated macrophages increased neuronal calcium influx acutely, followed by a delayed calcium influx that persisted throughout the experiment. Addition of the MMP-9 specific inhibitor suppressed the delayed rise in calcium while having no effect on the acute response

suppressed by the addition of MMP-9 inhibitor I (Fig. 11). These data suggest that MMP-9 secretion from macrophages may be involved in the calcium destabilization and subsequent neurotoxicity seen during HIV exposure.

It is worth noting, in addition to modification of the effects of HIV, NGF in particular also exerted effects that were independent of HIV actions. Twenty proteins changed in response to HIV+NGF and showed high, largely negative, correlations with toxicity (Fig. 12). Decreases were seen in many growth related proteins (G-CSF R, GM-CSF R, M-CSF, M-CSF R, GDNF, NT-4, IGFBP-3, IGFBP-6, FGF-7, crypto-1, PDGF-AA and PDGF-BB) indicating a strong role for NGF in the regulation of growth factor secretion. Additional proteins influenced by NGF included osteoprotegerin, sgp130, IL-15, IL-19, CCL-16, LFA-1 alpha, HCR and SCF. An increase in CXCR1 was the only change associated with proNGF reflecting the low overall effect of proNGF on HIV-induced protein secretion. An additional 59 proteins were altered by HIV+NGF and 7 proteins for proNGF+HIV, relative to untreated cells but showed low correlations with toxicity. Notable protein changes in this category were decreases in IL-10, MIP-1alpha, GDF-9, TGF- $\beta$ 2, TGF- $\beta$ 3, IGFBP-1, MMP-1, and MMP-12 and increases in IL-15, IL-23 and MMP-11. An

**Fig. 12** NGF decreased a number of growth factors which showed mostly negative correlations to calcium destabilization. Values represent the change in fluorescence signal intensity on the protein array for HIV, NGF+HIV or proNGF+HIV treated cells relative to matched control medium collected prior to stimulation. In most cases the effect of NGF was independent of HIV (little or no effect of HIV)



increase in NGF was also seen, most likely representing the NGF added to the culture.

## Discussion

### HIV Induces a Unique Neurotoxic Phenotype in hMDM

Macrophage activation is a key correlate of damage severity during HIV neuropathogenesis. Previous studies have clearly established the role of macrophage secretory products in HIV neuropathogenesis (Giulian et al. 1990; Pulliam et al. 1991b) but the cellular mechanisms that control toxin secretion are not fully understood. This lack of understanding has been a significant hurdle for the development of interventions that could control the damaging effects of inflammation. In this study we showed that macrophage activation and neurotoxin secretion induced by non-infectious HIV virions is accompanied by a unique phenotype that was similar to the phenotype seen in a previous study with proNGF stimulation (Williams et al. 2015). The secretion of factors that disrupted calcium regulation and induced the formation of varicosities in cultured neurons correlated with the appearance of distinct actin rich structures in hMDM. Macrophage conditioned medium from cultures possessing cells rich in podosomes resulted in higher neurotoxicity compared to cultures expressing predominately ruffled cells. These observations are similar to studies showing that the HIV protein, Nef, induced podosome formation (Verollet et al. 2015). The authors concluded that the induction of podosomes may facilitate migration of macrophages into tissues. This possibility is supported by our results showing that HIV virions stimulated both podosome formation and increased migration of macrophages through a Matrigel barrier. These data also indicate that neurotoxin secretion is associated with functional modifications of the actin cytoskeleton.

Calcium spiking in macrophages has been correlated with membrane ruffling (Kruskal and Maxfield 1987; Ohsawa et al. 2000; Myers and Swanson 2002; Patel and Harrison 2008)

although the function of the spiking is not well understood. The higher spike frequency in hMDM with ruffles versus podosomes is consistent with these previous observations. The suppression of these spikes by HIV following a small acute calcium response may be due in part to the loss of cells containing membrane ruffles (shifting to podosome expression) but could also reflect the loss of specific receptors or ligands that mediate the calcium response. Further studies are needed to identify the functions associated with calcium spikes in macrophages.

### Neurotrophins Differentially Regulate HIV-Induced Macrophage Functions

Given the many similarities between HIV stimulation of macrophages and results seen in a previous study exploring proNGF's effects on macrophages, we show for the first time that pro versus mature neurotrophin signaling can differentially regulate HIV induced macrophage phenotypes. An increase in the pro-neurotrophin to mature neurotrophin ratio in the CNS has been implicated in the pathogenesis of neurodegenerative diseases such as Alzheimer disease (Peng et al. 2004; Capsoni et al. 2011; Belrose et al. 2014) and has been demonstrated in the hippocampus of HIV-gp120 transgenic mice (Lee et al. 2013). While much of the work assessing the impact of pro and mature neurotrophin imbalance has been done in the context of neuronal damage, it is now clear that macrophages are significant targets of the neurotrophins largely due to expression of the p75<sup>NTR</sup> and TrkA. Blocking TrkA signaling enhanced neurotoxin production in response to HIV, while blocking the p75<sup>NTR</sup> reduced neurotoxin production and the formation of podosomes. Our studies showed that HIV induced a modest increase in the co-localization of the p75<sup>NTR</sup> with another known signaling partner, sortilin. High affinity binding of proNGF to the p75<sup>NTR</sup>/sortilin complex has been associated with cell death but no cell death was seen with HIV exposure, suggesting another potential role for sortilin in hMDM. Studies with the sortilin ligand neurotensin have reported an association with modifications of the cytoskeleton (Martin et al. 2005). The relationship between the p75<sup>NTR</sup> and podosome formation in our studies indicate that this may be a fruitful area for future studies.

When combined with HIV, proNGF did not alter or synergize with many of the phenotypic effects of HIV stimulation although it increased neurotoxicity of the conditioned medium. In contrast, NGF reduced or eliminated each of the major effects of HIV. Calcium spikes were greatly increased, podosome expression was reduced, the secretory profile was normalized and most importantly, toxin generation was suppressed, providing a novel avenue for controlling macrophage phenotype during HIV exposure.

### HIV and the hMDM Secretome

Analysis of the secretory profile of hMDM revealed patterns suggestive of a functional switch in response to HIV and the neurotrophins. Although cytokines did not clearly match an M1 or M2 profile, HIV did increase cytokines and chemokines that have previously been shown to be increased by HIV, including MCP-1, MIP1b, and MIP-2 (Del Corno et al. 2001). In addition, many changes were seen in growth factors which, highlights the importance of assessing potential loss of protection as well as detrimental responses of macrophages. To establish a link between each protein in the hMDM secretome and neurotoxicity, each condition was correlated with the corresponding neuronal calcium destabilization. Proteins with a strong positive or negative correlation were grouped by function to determine if a particular functional phenotype was related to the toxicity.

One of the functional associations found in this protein analysis was the angiogenic factor family where the changes induced by HIV favored an anti-angiogenic like profile. Although not all proteins associated with angiogenesis fit this profile the strong trend indicated a functional shift that has not yet been explored. Much of the work done on angiogenesis has been in the context of Kaposi sarcoma, an angioproliferative mesenchymal cancer often seen in AIDS and other immune deficient patients. HIV Tat and nef have been shown to promote Kaposi sarcoma induced angiogenesis (Zhou et al. 2013, 2014). The anti-angiogenic factor thrombospondin-1 inhibits HIV-Kaposi sarcoma induced angiogenic activity (Taraboletti et al. 1999). In our studies, thrombospondin and thrombospondin -1 were increased with HIV while angiostatin and thrombospondin-2 were reduced suggesting that macrophages may respond to HIV by regulating key angiogenic factors. ProNGF co-stimulation of macrophages with HIV increased the secretion of thrombospondin, thrombospondin-1, and angiostatin. This increase in anti-angiogenic factors induced by proNGF indicated that there may be a role for p75<sup>NTR</sup> in anti-angiogenesis which could synergize with HIV. This is consistent with a study that showed p75<sup>NTR</sup> expression was upregulated in endothelial cells of type one diabetic mice and was involved in inhibiting neovascularization (Caporali et al. 2008). These findings suggest an important role for proNGF signaling in macrophages during cancer prevention including HIV-induced Kaposi sarcoma. In contrast, co-stimulation of hMDMs with NGF reversed the secretion of all anti-angiogenic factors induced by HIV. This is consistent with many studies implicating a role for NGF in promoting angiogenesis (Nico et al. 2008).

The TGF and FGF families were highly affected by HIV; however, not much is known about these families in the context of HIV. The most robust changes came from the GDF subgroup of the TGF family. GDF3, GDF5 and GDF9 were robustly secreted by the hMDM but little is known about their function.

GDF3 was the only member of this subgroup that correlated with toxicity although a positive relationship with correlations slightly below the significance cutoff (0.56–0.67) was seen for other GDFs, suggesting a potential relationship between this protein group and toxicity. Although the positive correlation would suggest a role in toxicity it remains to be determined if the changes are compensatory or causal. Likewise, in the FGF family, FGF-9 in particular was increased by HIV and the increase was reversed by NGF. FGF-9 has been shown to be secreted from neurons and to support survival of basal forebrain cholinergic neurons (Kanda et al. 2000). However, more work needs to be done to understand the importance of these factors in the context of HIV neuropathogenesis.

Although significant correlations were identified, the results from the protein arrays provided few leads that might identify the protein(s) responsible for neurotoxicity. The strongest candidates from these studies were proteins within the MMP family. One of the most striking observations from the protein array analysis was the increase in MMP-9 and the tissue inhibitor of metalloprotease-1 (TIMP-1) in response to HIV. Both proteins were robustly expressed and had strong positive correlations to calcium dysregulation. The increase in MMP-9 correlated with the expression of podosomes consistent with studies showing a link between this structural phenotype and MMP-9 secretion (Varon et al. 2006; Burger et al. 2011). In HIV infected patients, MMP-9 is elevated in the CSF suggesting a role for MMP-9 in HIV induced neurotoxicity (Conant et al. 1999; Kanda et al. 2000; Ohsawa et al. 2004; Russo et al. 2007). In this study we showed that inhibition of MMP-9 activity in macrophage conditioned medium suppressed the delayed calcium deregulation. MMP-9 itself recapitulated some but not all of the effects of the conditioned medium (unpublished observations). However, the increased secretion of both MMP-9 and its endogenous inhibitor TIMP-1 indicated that the hMDM secrete potentially deleterious and protective proteins at the same time in an effort to maintain tissue homeostasis. The balance between MMP-9 and TIMP-1 has been seen in other brain injury models including ALS (Louboutin et al. 2011; Tsai et al. 2011; Fischer et al. 2013; Wu et al. 2015) and may be a crucial factor in the regulation of tissue damage. Evidence for deleterious effects when the balance is changed was seen when proNGF was added to HIV. A decrease in the secretion of TIMP-1 resulted which corresponded to the increase in neurotoxicity. This is in contrast to the partially protective role of NGF which could also be explained by its ability to suppress HIV-induced MMP-9 secretion. In addition, MMP-9 may have deleterious effects related to its ability to metabolize NGF (Bruno and Cuello 2006), creating a favorable environment for a high ratio of proNGF to mature NGF. The consistency of these observations makes MMP-9 a putative candidate for the neurotoxin, however, additional work is needed to understand how MMP-9 may be involved in HIV induced neuropathogenesis.

## Conclusion

These studies describe the functional macrophage phenotype induced by HIV characterized by the expression of podosomes, suppression of calcium spiking and increased neurotoxin production. Proteins showing the most robust changes in the macrophage conditioned medium in response to HIV included growth factors and MMP-9. Co-stimulation with NGF suppressed the HIV-induced neurotoxic phenotype in macrophages, increased calcium spiking, suppressed podosome expression and reversed many of the protein secretory changes, including MMP-9. In contrast, co-stimulation of macrophages with proNGF not only failed to reverse the effects of HIV but increased the neurotoxic phenotype. The opposing effects of NGF and proNGF were consistent with actions at TrkA and p75<sup>NTR</sup>, respectively. Blockade of p75<sup>NTR</sup> signaling suppressed the formation of podosomes and neurotoxin production whereas blockade of TrkA signaling enhanced toxicity. These differential effects of proNGF and NGF on macrophage activation by HIV reveal novel mechanisms that may be exploited for the therapeutic control of macrophage activation in response to HIV and other neurodegenerative conditions.

**Acknowledgments** This research was supported by NIH grants: F31 MH101019, R01 MH085606 and R01 NS083164.

**Conflict of Interest** The authors declare that they have no conflict of interest.

**Ethical Approvals** All animal work was done in accordance with NIH animal welfare guidelines and was approved by the University of North Carolina-Chapel Hill Institutional Animal Care and Use Committee board (approval number 14–147.0).

No human participants were used in these studies.

For the macrophage cultures, human buffy coat leukocytes were purchased and shipped within 24 h after blood draw from healthy donors at the New York Blood Center (<http://nybloodcenter.org/>), a non-profit organization for the collection and distribution of blood for clinical and research purposes. All research use was screened by the center and no personal identifiers were sent with the shipment. Such use is exempt from review under NIH guidelines, exemption 4 of 46-101 (b).

## References

- Al-Shawi R, Hafner A, Chun S, Raza S, Crutcher K, Thrasyvoulou C, Simons P, Cowen T (2007) ProNGF, sortilin, and age-related neurodegeneration. *Ann N Y Acad Sci* 1119:208–215
- Belrose JC, Masoudi R, Michalski B, Fahnestock M (2014) Increased pro-nerve growth factor and decreased brain-derived neurotrophic factor in non-Alzheimer's disease tauopathies. *Neurobiol Aging* 35: 926–933
- Bruno MA, Cuello AC (2006) Activity-dependent release of precursor nerve growth factor, conversion to mature nerve growth factor, and its degradation by a protease cascade. *Proc Natl Acad Sci U S A* 103:6735–6740

- Burger KL, Davis AL, Isom S, Mishra N, Seals DF (2011) The podosome marker protein Tks5 regulates macrophage invasive behavior. *Cytoskeleton (Hoboken)* 68:694–711
- Caporali A, Pani E, Horrevoets AJ, Kraenkel N, Oikawa A, Sala-Newby GB, Meloni M, Cristofaro B, Graiani G, Leroyer AS, Boulanger CM, Spinetti G, Yoon SO, Madeddu P, Emanuelli C (2008) Neurotrophin p75 receptor (p75NTR) promotes endothelial cell apoptosis and inhibits angiogenesis: implications for diabetes-induced impaired neovascularization in ischemic limb muscles. *Circ Res* 103:e15–26
- Capsoni S, Brandi R, Arisi I, D’Onofrio M, Cattaneo A (2011) A dual mechanism linking NGF/proNGF imbalance and early inflammation to Alzheimer’s disease neurodegeneration in the AD11 anti-NGF mouse model. *CNS Neurol Disord Drug Targets* 10:635–647
- Conant K, McArthur JC, Griffin DE, Sjulson L, Wahl LM, Irani DN (1999) Cerebrospinal fluid levels of MMP-2, 7, and 9 are elevated in association with human immunodeficiency virus dementia. *Ann Neurol* 46:391–398
- da Huang W, Sherman BT, Lempicki RA (2009a) Bioinformatics enrichment tools: paths toward the comprehensive functional analysis of large gene lists. *Nucleic Acids Res* 37:1–13
- da Huang W, Sherman BT, Lempicki RA (2009b) Systematic and integrative analysis of large gene lists using DAVID bioinformatics resources. *Nat Protoc* 4:44–57
- Del Corno M, Liu QH, Schols D, de Clercq E, Gessani S, Freedman BD, Collman RG (2001) HIV-1 gp120 and chemokine activation of Pyk2 and mitogen-activated protein kinases in primary macrophages mediated by calcium-dependent, pertussis toxin-insensitive chemokine receptor signaling. *Blood* 98:2909–2916
- Fischer M, Dietmann A, Beer R, Broessner G, Helbok R, Pfausler B, Schmutzhard E, Lackner P (2013) Differential regulation of matrix-metalloproteinases and their tissue inhibitors in patients with aneurysmal subarachnoid hemorrhage. *PLoS One* 8, e59952
- Fischer-Smith T, Tedaldi EM, Rappaport J (2008) CD163/CD16 coexpression by circulating monocytes/macrophages in HIV: potential biomarkers for HIV infection and AIDS progression. *AIDS Res Hum Retrovir* 24:417–421
- Garaci E, Caroleo MC, Aloe L, Aquaro S, Piacentini M, Costa N, Amendola A, Micera A, Calio R, Perno CF, Levi-Montalcini R (1999) Nerve growth factor is an autocrine factor essential for the survival of macrophages infected with HIV. *Proc Natl Acad Sci U S A* 96:14013–14018
- Giulian D, Vaca K, Noonan CA (1990) Secretion of neurotoxins by mononuclear phagocytes infected with HIV-1. *Science* 250:1593–1596
- Harrold SM, Dragic JM, Brown SL, Achim CL (2001) Neurotrophic factor regulation of human immunodeficiency virus type 1 replication in human blood-derived macrophages through modulation of coreceptor expression. *Adv Exp Med Biol* 493:41–47
- Ibanez CF (2002) Jekyll-Hyde neurotrophins: the story of proNGF. *Trends Neurosci* 25:284–286
- Johnston JB, Zhang K, Silva C, Shalinsky DR, Conant K, Ni W, Corbett D, Yong VW, Power C (2001) HIV-1 Tat neurotoxicity is prevented by matrix metalloproteinase inhibitors. *Ann Neurol* 49:230–241
- Kanda T, Iwasaki T, Nakamura S, Kurokawa T, Ikeda K, Mizusawa H (2000) Self-secretion of fibroblast growth factor-9 supports basal forebrain cholinergic neurons in an autocrine/paracrine manner. *Brain Res* 876:22–30
- Kaul M, Lipton SA (1999) Chemokines and activated macrophages in HIV gp120-induced neuronal apoptosis. *Proc Natl Acad Sci U S A* 96:8212–8216
- Kolson DL (2002) Neuropathogenesis of central nervous system HIV-1 infection. *Clin Lab Med* 22:703–717
- Kruskal BA, Maxfield FR (1987) Cytosolic free calcium increases before and oscillates during frustrated phagocytosis in macrophages. *J Cell Biol* 105:2685–2693
- Laskin DL, Sunil VR, Gardner CR, Laskin JD (2011) Macrophages and tissue injury: agents of defense or destruction? *Annu Rev Pharmacol Toxicol* 51:267–288
- Lee R, Kermani P, Teng KK, Hempstead BL (2001) Regulation of cell survival by secreted proneurotrophins. *Science* 294:1945–1948
- Lee MH, Amin ND, Venkatesan A, Wang T, Tyagi R, Pant HC, Nath A (2013) Impaired neurogenesis and neurite outgrowth in an HIV-gp120 transgenic model is reversed by exercise via BDNF production and Cdk5 regulation. *J Neurovirol* 19:418–431
- Liuzzi GM, Mastroianni CM, Santacroce MP, Fanelli M, D’Agostino C, Vullo V, Riccio P (2000) Increased activity of matrix metalloproteinases in the cerebrospinal fluid of patients with HIV-associated neurological diseases. *J Neurovirol* 6:156–163
- Longo FM, Yang T, Knowles JK, Xie Y, Moore LA, Massa SM (2007) Small molecule neurotrophin receptor ligands: novel strategies for targeting Alzheimer’s disease mechanisms. *Curr Alzheimer Res* 4:503–506
- Louboutin JP, Reyes BA, Agrawal L, Van Bockstaele EJ, Strayer DS (2011) HIV-1 gp120 upregulates matrix metalloproteinases and their inhibitors in a rat model of HIV encephalopathy. *Eur J Neurosci* 34:2015–2023
- Martin S, Dicou E, Vincent JP, Mazella J (2005) Neurotensin and the neurotensin receptor-3 in microglial cells. *J Neurosci Res* 81:322–326
- Meeker RB, Poulton W, Markovic-Plese S, Hall C, Robertson K (2011) Protein changes in CSF of HIV-infected patients: evidence for loss of neuroprotection. *J Neurovirol* 17:258–273
- Mocchetti I, Bachis A (2004) Brain-derived neurotrophic factor activation of TrkB protects neurons from HIV-1/gp120-induced cell death. *Crit Rev Neurobiol* 16:51–57
- Mocchetti I, Nosheny RL, Tanda G, Ren K, Meyer EM (2007) Brain-derived neurotrophic factor prevents human immunodeficiency virus type 1 protein gp120 neurotoxicity in the rat nigrostriatal system. *Ann N Y Acad Sci* 1122:144–154
- Mufson EJ, Counts SE, Fahnestock M, Ginsberg SD (2007) Cholinergic molecular substrates of mild cognitive impairment in the elderly. *Curr Alzheimer Res* 4:340–350
- Myers JT, Swanson JA (2002) Calcium spikes in activated macrophages during Fcγ receptor-mediated phagocytosis. *J Leukoc Biol* 72:677–684
- Nico B, Mangieri D, Benaglio V, Crivellato E, Ribatti D (2008) Nerve growth factor as an angiogenic factor. *Microvasc Res* 75:135–141
- Ohsawa K, Imai Y, Kanazawa H, Sasaki Y, Kohsaka S (2000) Involvement of Iba1 in membrane ruffling and phagocytosis of macrophages/microglia. *J Cell Sci* 113(Pt 17):3073–3084
- Ohsawa K, Imai Y, Sasaki Y, Kohsaka S (2004) Microglia/macrophage-specific protein Iba1 binds to fimbrin and enhances its actin-bundling activity. *J Neurochem* 88:844–856
- Patel PC, Harrison RE (2008) Membrane ruffles capture C3bi-opsonized particles in activated macrophages. *Mol Biol Cell* 19:4628–4639
- Peng S, Wu J, Mufson EJ, Fahnestock M (2004) Increased proNGF levels in subjects with mild cognitive impairment and mild Alzheimer disease. *J Neuropathol Exp Neurol* 63:641–649
- Pulliam L, Herndier B, Tang N, McGrath M (1991a) Human immunodeficiency virus-infected macrophages produce soluble factors that cause histological and neurochemical alterations in cultured human brains. *J Clin Invest* 87:506–512
- Pulliam L, Herndier BG, Tang NM, McGrath MS (1991b) Human immunodeficiency virus-infected macrophages produce soluble factors that cause histological and neurochemical alterations in cultured human brains. *J Clin Invest* 87:503–512
- Reichardt LF (2006) Neurotrophin-regulated signalling pathways. *Philos Trans R Soc Lond Ser B Biol Sci* 361:1545–1564

- Rossio JL, Esser MT, Suryanarayana K, Schneider DK, Bess JW Jr, Vasquez GM, Wiltout TA, Chertova E, Grimes MK, Sattentau Q, Arthur LO, Henderson LE, Lifson JD (1998) Inactivation of human immunodeficiency virus type 1 infectivity with preservation of conformational and functional integrity of virion surface proteins. *J Virol* 72:7992–8001
- Russo R, Siviglia E, Gliozzi M, Amantea D, Paoletti A, Berliocchi L, Bagetta G, Corasaniti MT (2007) Evidence implicating matrix metalloproteinases in the mechanism underlying accumulation of IL-1 $\beta$  and neuronal apoptosis in the neocortex of HIV/gp120-exposed rats. *Int Rev Neurobiol* 82:407–421
- Samah B, Porcheray F, Gras G (2008) Neurotrophins modulate monocyte chemotaxis without affecting macrophage function. *Clin Exp Immunol* 151:476–486
- Samah B, Porcheray F, Dereuddre-Bosquet N, Gras G (2009) Nerve growth factor stimulation promotes CXCL-12 attraction of monocytes but decreases human immunodeficiency virus replication in attracted population. *J Neurovirol* 15:71–80
- Shi J, Longo FM, Massa SM (2013) A small molecule p75(NTR) ligand protects neurogenesis after traumatic brain injury. *Stem Cells* 31:2561–2574
- Streit WJ (2005) Microglia and neuroprotection: implications for Alzheimer's disease. *Brain Res Brain Res Rev* 48:234–239
- Taraboletti G, Benelli R, Borsotti P, Rusnati M, Presta M, Giavazzi R, Ruco L, Albini A (1999) Thrombospondin-1 inhibits Kaposi's sarcoma (KS) cell and HIV-1 Tat-induced angiogenesis and is poorly expressed in KS lesions. *J Pathol* 188:76–81
- Tsai HC, Ye SY, Kunin CM, Lee SS, Wann SR, Tai MH, Shi MH, Liu YC, Chen YS (2011) Expression of matrix metalloproteinases and their tissue inhibitors in the serum and cerebrospinal fluid of patients with HIV-1 infection and syphilis or neurosyphilis. *Cytokine* 54:109–116
- Varon C, Tatin F, Moreau V, Van Obberghen-Schilling E, Fernandez-Sauze S, Reuzeau E, Kramer I, Genot E (2006) Transforming growth factor beta induces rosettes of podosomes in primary aortic endothelial cells. *Mol Cell Biol* 26:3582–3594
- Verollet C, Souriant S, Bonnaud E, Jolicoeur P, Raynaud-Messina B, Kinnaer C, Fourquaux I, Imle A, Benichou S, Fackler OT, Poincloux R, Maridonneau-Parini I (2015) HIV-1 reprograms the migration of macrophages. *Blood* 125:1611–1622
- Williams KS, Killebrew DA, Clary GP, Seawell JA, Meeker RB (2015) Differential regulation of macrophage phenotype by mature and proneurotrophin growth factor. *J Neuroimmunol* 285:76–93
- Wu J, Zhao D, Wu S, Wang D (2015) Ang-(1–7) exerts protective role in blood–brain barrier damage by the balance of TIMP-1/MMP-9. *Eur J Pharmacol* 748:30–36
- Yang T, Knowles JK, Lu Q, Zhang H, Arancio O, Moore LA, Chang T, Wang Q, Andreasson K, Rajadas J, Fuller GG, Xie Y, Massa SM, Longo FM (2008) Small molecule, non-peptide p75 ligands inhibit Abeta-induced neurodegeneration and synaptic impairment. *PLoS One* 3, e3604
- Zhou F, Xue M, Qin D, Zhu X, Wang C, Zhu J, Hao T, Cheng L, Chen X, Bai Z, Feng N, Gao SJ, Lu C (2013) HIV-1 Tat promotes Kaposi's sarcoma-associated herpesvirus (KSHV) vIL-6-induced angiogenesis and tumorigenesis by regulating PI3K/PTEN/AKT/GSK-3 $\beta$  signaling pathway. *PLoS One* 8, e53145
- Zhu X, Guo Y, Yao S, Yan Q, Xue M, Hao T, Zhou F, Zhu J, Qin D, Lu C (2014) Synergy between Kaposi's sarcoma-associated herpesvirus (KSHV) vIL-6 and HIV-1 Nef protein in promotion of angiogenesis and oncogenesis: role of the AKT signaling pathway. *Oncogene* 33:1986–1996